Aust. J. Phys., 1995, **48**, 571–612

Pulsars with Strong Magnetic Fields: Polar Gaps, Bound Pair Creation and Nonthermal Luminosities

V. V. Usov[A] *and D. B. Melrose*[B]

[A] Physics Department, Weizmann Institute, Rehovot 76100, Israel.
[B] Research Centre for Theoretical Astrophysics, School of Physics, University of Sydney, NSW 2006, Australia.

Abstract

Modifications to polar-gap models for pulsars are discussed for the case where the surface magnetic field, B_s, of the neutron star is strong. For $B \geq 4 \times 10^8$ T, the curvature γ-quanta emitted tangentially to the curved force lines of the magnetic field are captured near the threshold of bound pair creation and are channelled along the magnetic field as bound electron–positron pairs (positronium). The stability of such bound pairs against ionization by the parallel electric field, $E_\parallel$, in the polar cap, and against photoionization is discussed. Unlike free pairs, bound pairs do not screen $E_\parallel$ near the neutron star. As a consequence, the energy flux in highly relativistic particles and high-frequency (X-ray and/or γ-ray) radiation from the polar gaps can be much greater than in the absence of positronium formation. We discuss this enhancement for (a) Arons-type models, in which particles flow freely from the surface, and find any enhancement to be modest, and (b) Ruderman–Sutherland-type models, in which particles are tightly bound to the surface, and find that the enhancement can be substantial. In the latter case we argue for a self-consistent model in which partial screening of $E_\parallel$ maintains it close to the threshold value for field ionization of the bound pairs, and in which a reverse flux of accelerated particles maintains the polar cap at a temperature such that thermionic emission supplies the particles needed for this screening. This model applies only in a restricted range of periods, $P_2 < P < P_1$, and it implies an energy flux in high-energy particles that can correspond to a substantial fraction of the spin-down power of the pulsar.

Nonthermal, high-frequency radiation has been observed from six radio pulsars and Geminga is usually included as a seventh case. The nonthermal luminosity can be higher than can be explained in terms of conventional polar-gap and outer-gap models. The self-consistent polar-gap model proposed here alleviates this difficulty, provided the magnetic field satisfies $B \gtrsim 4 \times 10^8$ T (which is so for five of these pulsars, and plausibly for the other two if a modest nondipolar component is assumed), and the surface temperature (in the absence of heating by the reverse flux) satisfies $T_s \lesssim 0{\cdot}5 \times 10^6$ K, so that thermionic emission from the surface is unimportant. It is argued that sufficient power is available to explain the observed high-frequency radiation of most of these pulsars. However, the Crab and PSR 0540–69 have periods $P < P_2$, and we suggest that an outer-gap model is more appropriate for these. Our model implies a death line at $P = P_1 \sim 0{\cdot}5$ s for $B \gtrsim 4 \times 10^8$ T, and we speculate on why, nevertheless, radio pulsars with strong fields are found at $P > P_1$.

1. Introduction

The creation of electron–positron pairs by decay of γ rays as they propagate across magnetic field lines is an essential ingredient in the population of a pulsar magnetosphere with plasma. In the absence of plasma, a strong electric field $\mathbf{E}$ results from the rotation of the magnetized neutron star (Goldreich and Julian 1969). The vacuum field has a nonzero parallel component $E_\parallel = (\mathbf{E} \cdot \mathbf{B})/|\mathbf{B}|$

0004-9506/95/040571$15.00

along the magnetic field $\mathbf{B}$, and this $E_\parallel$ can accelerate *primary* particles to ultrarelativistic energies (e.g., the review by Michel 1991). The source of the primary particles is different in different models. In the absence of free ejection from the stellar surface, the primary particles come from a pair cascade initiated, for example, by decay of stray γ rays into pairs (Ruderman and Sutherland 1975). In such models the vacuum $E_\parallel$ is present immediately above the surface and is said to form a vacuum gap. In models with free ejection of particles from the stellar surface, these particles screen $E_\parallel$ immediately above the surface, and set up the corotation electric field $\mathbf{E}_{\rm rot} = -(\mathbf{\Omega} \times \mathbf{r}) \times \mathbf{B}$, where $\mathbf{\Omega}$ is the angular velocity of rotation. The divergence of $\mathbf{E}_{\rm rot}$ requires a charge density, $en_{\rm GJ}$, where $n_{\rm GJ}$ is the Goldreich–Julian (1969) density. In such models an $E_\parallel$ develops, forming a vacuum-gap-like region above the surface, due to the actual charge density deviating increasingly with increasing height from the Goldreich–Julian value, $n \neq n_{\rm GJ}$. In either model, the primary particles emit γ rays, due to curvature emission and other processes. Some of these γ rays are absorbed in the magnetic field by creating free electron–positron pairs ($\gamma + B \rightarrow e^+ + e^- + B$). Provided these *secondary* particles are created in the gap, the $E_\parallel$ field can accelerate the electron and the positron in opposite directions, allowing a net charge density to build up, and it is this charge density of the secondary particles that screens $E_\parallel$. Regions where $E_\parallel$ is unscreened are called gaps, and a gap that forms near the magnetic poles of the pulsar is called a *polar gap*. The height, H, of a polar gap is defined by the height above the stellar surface where the charge density due to the charge-separated pairs is sufficient to screen $E_\parallel$. Besides polar-gap models there are also outer-gap models (e.g., Cheng, Ho and Ruderman 1986*a*,*b*), where the region with $E_\parallel \neq 0$ occurs far from the stellar surface, where the magnetic field is much weaker than in the polar-cap regions. In comparing the slot-gap with polar-gap and outer-gap models, we note that the slot gaps form on the boundary of the closed B-field region (Arons 1983). Primary particles which are ejected from the neutron star surface and are accelerated in the slot gap gain the main part of their energy far from the neutron star. In this respect, slot gaps differ significantly from the polar gaps and may be regarded as intermediate between polar gaps and outer gaps.

Polar gaps are thought to be a source of the energy for nonthermal radiation of pulsars (Sturrock 1971; Ruderman and Sutherland 1975; Michel 1975; Arons 1979, 1981; Arons and Scharlemann 1979; Cheng and Ruderman 1980; Mestel 1981, 1993; Mestel *et al.* 1985; Fitzpatrick and Mestel 1988*a*, *b*; Shibata 1991). In particular, in most models the radio emission is attributed to processes in polar gaps. However, the radio luminosities of the pulsars are small compared with the total power loss estimated from the observed spin down and associated rotational energy loss ($\lesssim 10^{-5}$). Most of the power loss is attributed to relativistic particles created as secondary pairs in the polar gaps and escaping in a relativistic wind (Ruderman and Sutherland 1975; Arons 1979; Michel 1991). In most pulsars the only nonthermal radiation observed is in the radio range and, apart from the slowing down, the large inferred power loss has no direct observational signature. However, there are a few radio pulsars that do have high-frequency emission (in X rays and/or γ rays, we do not distinguish between them in this paper) with a nonthermal luminosity that is a substantial fraction of the inferred rotational power loss. Nonthermal high-frequency radiation requires high energy particles,

and it is widely assumed that the high-frequency luminosity correlates with the power in primary particles (e.g., Harding and Daugherty 1993). The power in the primary particles, $\dot{N}_{\rm prim} e\Delta\varphi$, is limited by the rate of injection of such particles, $\dot{N}_{\rm prim}$, which is less than $n_{\rm GJ}c$ times the area of the polar cap, and the potential energy, $e\Delta\varphi \sim eE_{\|}H$, that particles gain in crossing the polar gap. The maximum potential difference across the polar gap is when there is no screening at all:

$$\Delta\varphi_{\rm max} = \frac{\Omega^2 B_{\rm s}^{\rm d} R^3}{2c^2} \simeq (6{\cdot}6 \times 10^{14}\,{\rm V})\left(\frac{B_{\rm s}^{\rm d}}{10^8\,{\rm T}}\right)\left(\frac{P}{0{\cdot}1\,{\rm s}}\right)^{-2}, \qquad (1{\cdot}1)$$

where $B_{\rm s}^{\rm d}$ is the dipole component of the magnetic field at the magnetic pole on the neutron star surface, $\Omega = 2\pi/P$ is the angular speed of rotation of the neutron star and $R \simeq 10^4$ m is the radius of the neutron star. For $\Delta\varphi = \Delta\varphi_{\rm max}$ the implied maximum value for power of primary particles is equal (within a factor of order unity) to the rotational energy loss. For existing polar-gap models the value of $\Delta\varphi$ is considerably less than $\Delta\varphi_{\rm max}$. In Arons-type models, in which particles flow freely from the surface, this is due both (a) to $E_{\|}$ being much less than the vacuum value due to screening by the primary particles that flow freely from the surface, and (b) to the height being less than the maximum value, $H \sim \Delta R_p$ where ΔR_p is the radius of the polar cap, due to screening by secondary pairs. In Ruderman–Sutherland-type models, in which particles are tightly bound to the surface, $\Delta\varphi = \Delta\varphi_{\rm max}$ results from $H \ll \Delta R_p$ due to screening by secondary pairs.

Strong high-frequency radiation is observed from the galactic pulsars PSR 0531+21, PSR 0833–45, PSR 1055–52, PSR 1509–58 and PSR 1706–44, and PSR 0540–69 in the Large Magellanic Cloud (e.g., the review by Ulmer 1994). The observed radiated power for all these pulsars is concentrated in the X-ray or γ-ray ranges. The γ-ray pulsar Geminga is probably also a radio pulsar (Halpern and Holt 1992) which is 'radio quiet' because its radio beam does not intersect the Earth (Ozernoy and Usov 1977). The high γ-ray luminosities are inferred assuming emission into a large solid angle, $\sim 2\pi$ sterad (Ulmer 1994). For some of the the pulsars, notably for PSR 1055–52, among the present polar-gap models the only one that appears capable of explaining the inferred very high luminosities is that of Sturrock (1971). In the Sturrock model the potential drop has the maximum possible value, and the nonthermal power is of the order of the rotational power loss. However, the Sturrock model is not self-consistent because it neglects the finite limit on the height of the polar gap due to screening. In the Sturrock model the free electron–positron pairs created by the curvature γ-quanta inside the polar gap are assumed not to feel the electric field $E_{\|}$ and not to screen this field so that the full potential drop $\Delta\varphi_{\rm max}$ is implicitly available. This internal inconsistency implies that the Sturrock model should not be used for detailed estimates of the pulsar luminosities.

Ruderman and Sutherland (1975) were the first to develop a self-consistent polar-gap model in which the screening of the electric field $E_{\|}$ by the electron–positron pairs created in it is taken into account. Consideration of this screening led Ruderman and Sutherland (1975) to conclude that the potential across the

polar gap cannot exceed $\Delta\varphi_{\rm RS} \simeq$ a few $\times 10^{12}$ V. This upper limit on the potential across the polar gap is valid for any polar-gap model in which free pairs are created by γ-quanta absorption in the magnetic field. For young, rapidly-rotating pulsars with typical parameters, $P \lesssim 0{\cdot}1$ s and $B_{\rm s}^{\rm d} \gtrsim 10^8$ T, one has $\Delta\varphi_{\rm RS} \lesssim 10^{-3}\,\Delta\varphi_{\rm max}$. The total power in primary particles is proportional to $\Delta\varphi$, and the maximum luminosity expected in all existing polar-gap models (Ruderman and Sutherland 1975; Arons 1979, 1981; Arons and Scharlemann 1979; Cheng and Ruderman 1980; Mestel *et al.* 1985) is smaller than the inferred nonthermal luminosity in X-rays and γ rays (Section 5).

In all existing polar-gap models, the formation of pairs in the pulsar magnetospheres is due to the single-photon mechanism, $\gamma + B \rightarrow e^+ + e^- + B$, and the resulting pairs are free. However, this assumption that the pairs are free is not valid if the magnetic field is strong enough, specifically for $B > 0{\cdot}1\,B_{\rm cr}$, where $B_{\rm cr} = m^2c^2/e\hbar = 4{\cdot}4 \times 10^9$ T is known as the critical field. In such a strong magnetic field, the curvature γ-quanta emitted tangentially to the curved force lines of the magnetic field are captured near the threshold of bound pair creation and are then channelled along the magnetic field as positronium, that is, as bound pairs (Shabad and Usov 1982, 1985, 1986; Herold, Ruder and Wunner 1985; Usov and Shabad 1985; Mészáros 1992; Shabad 1992 and references therein). This positronium may be stable in the polar gaps against both the ionizing action of the electric field and against photo-ionization (Shabad and Usov 1985; Bhatia, Chopra and Panchapakesan 1988, 1992). Unlike free pairs, such bound pairs do not screen the electric field $E_\parallel$ near the pulsar. Screening requires a net charge density, which can build up due to free pairs being separated by $E_\parallel$, but cannot build up if the pairs remain bound. As a result the height of the gap, which is determined by the height at which screening becomes important, is greater than it would be in the absence of formation of positronium. The assumption that the power in primary particles is proportional to H in polar-gap models implies that this total luminosity increases when positronium formation becomes important (Usov and Shabad 1985). We argue in Section 5 that the nonthermal luminosity may even become comparable with the maximum possible, as in the model of Sturrock (1971).

Our primary objective in this paper is to discuss how models of pulsar electrodynamics need to be modified when the magnetic field is strong enough for creation of bound pairs to dominate over the formation of free pairs. First, however, we review several important preliminary aspects of the problem. The rate of injection of the primary particles depends on the properties of the matter at the surface of a magnetic neutron star. The particle outflow from the neutron star surface is discussed in Section 2. Particle acceleration and generation of curvature γ rays in the pulsar magnetospheres are described in Section 3. Propagation of γ rays, including photon splitting, and creation of electron–positron pairs in a strong magnetic field are discussed in Section 4. In Section 5, the polar-gap model is developed for pulsars with strong magnetic fields at their surface, $B_{\rm s} > 0{\cdot}1\,B_{\rm cr}$, and the maximum value of the nonthermal luminosity is estimated for such a pulsar. The interpretation of the observational data and some theoretical predictions on the nonthermal radiation of pulsars with $B_{\rm s} > 0{\cdot}1\,B_{\rm cr}$ are also given in Section 5. A discussion and summary are presented in Section 6.

2. Neutron Star Surface and Particle Ejection

The electric field distribution and particle acceleration in the polar gaps of pulsars depend on the character of particle outflow from the pulsar surface. In some models the binding to the surface is assumed sufficiently strong that no particles are ejected from the surface, and in other models the binding is assumed sufficiently weak that particles (either electrons or ions) flow freely from the stellar surface. Particle ejection from the surface depends on the composition of the neutron star surface, the structure of the surface with a strong magnetic field and the surface temperature T_s. In this section, after a brief review of polar-gap models we discuss the properties of the stellar surface and their effect on the binding or ejection of ions. We then discuss models involving free ejection of electrons and free ejection of ions.

2.1 Polar-gap Models

There are several kinds of polar-gap model. These may be classified in two ways: whether ions or electrons tend to be ejected from the surface, and whether $E_\parallel$ is zero or nonzero at the stellar surface.

The sign of the charge of the particles that tend to be ejected from the neutron star surface depends on the sign of $\mathbf{\Omega} \cdot \mathbf{B}$. Electrons tend to be ejected for $\mathbf{\Omega} \cdot \mathbf{B} > 0$ and ions for $\mathbf{\Omega} \cdot \mathbf{B} < 0$. The argument for this (Goldreich and Julian 1969; Ruderman and Sutherland 1975; Arons 1979, 1981) is that plasma tends to corotate with the star, and the divergence of the corotation electric field implies a charge density, en_{GJ}, where

$$n_{\mathrm{GJ}} = \frac{2\epsilon_0 |\Omega . \mathbf{B}|}{e} \simeq (7 \times 10^{17}\,\mathrm{m}^{-3}) \left(\frac{B}{10^8\,\mathrm{T}}\right) \left(\frac{P}{0{\cdot}1\,\mathrm{s}}\right)^{-1} \cos\theta\,, \qquad (2{\cdot}1)$$

is the Goldreich–Julian density, and θ is the angle between the angular velocity $\mathbf{\Omega}$ and the magnetic field $\mathbf{B}$. Thus the tendency to corotate requires positive charges above the polar caps for $\mathbf{\Omega} \cdot \mathbf{B} < 0$ and negative charges over the polar caps for $\mathbf{\Omega} \cdot \mathbf{B} > 0$. The required charge density may be produced in two ways: ejection of particles with the appropriate sign of the charge from the stellar surface, or acceleration (by $E_\parallel$) from the magnetosphere back to the stellar surface of charges of the opposite sign.

The most familiar model in which there is no ejection of particles from the stellar surface is that of Ruderman and Sutherland (1975). This model applies only to neutron stars with $\mathbf{\Omega} \cdot \mathbf{B} < 0$ (neutron stars with $\mathbf{\Omega} \cdot \mathbf{B} > 0$ are assumed not to be pulsars). The absence of ion flow from the surface is attributed to an assumed strong binding of iron nuclei. In the Ruderman–Sutherland model, the field $E_\parallel$ is maximum at the surface and decreases with distance. All the particles in the pulsar magnetosphere are created from pair production through γ-ray absorption in the polar gap. The magnetosphere is populated by a pair plasma created in the polar gap, and the (positive) Goldreich–Julian charge density is created by electrons being accelerated back to the stellar surface, leaving a net excess (and outward flux) of positrons. A model with somewhat similar properties is that of Beskin, Gurevich and Istomin (1986) in which the pair plasma is assumed to be created in a postulated double layer immediately above the surface on the star.

In contrast, in the model of Arons (1979, 1981) it is assumed that charged particles (electrons or ions depending on the sign of $\mathbf{\Omega} \cdot \mathbf{B}$) flow freely from the neutron star surface. In this model the electric field $E_{\|}$ is equal to zero at the surface, and increases with distance above the surface. In the absence of any additional source of charge, conservation of the current implies a current density $J \propto B$. For so-called *favourably* curved field lines, the ratio of the charge density ($n = J/ec \propto B$) to the Goldreich–Julian charge density ($n_{\rm GJ} \propto \mathbf{\Omega} \cdot \mathbf{B}/\Omega$) decreases with distance above the stellar surface. This implies that the screening of $E_{\|}$ is incomplete, and $E_{\|}$ increases toward the vacuum value. The resulting $E_{\|}$, which is smaller than that in the Ruderman–Sutherland model, causes the ejected electrons or ions to become highly relativistic and causes a net flux of pair-produced electrons or positrons back to the stellar surface to allow the charge density to be maintained at the Goldreich–Julian value. Mestel *et al.* (1985) pointed out that for the unfavourably curved field lines, along which $n/n_{\rm GJ}$ increases, an $E_{\|}$ of opposite sign to the vacuum field develops and plays essentially the same role as the $E_{\|}$ in the Arons model. A third kind of polar-gap model (Cheng and Ruderman 1980) is an intermediate case where the particles flow from the pulsar surface but not freely. In such a model the field $E_{\|}$ is nonzero at the pulsar surface but it is smaller than in the model of Ruderman and Sutherland (1975).

In the discussion below, we use the Ruderman–Sutherland and Arons models for illustrative purposes.

2·2 Composition of the Neutron Star Surface

The strength of the binding of ions to the stellar surface is an important ingredient in pulsar models with $\mathbf{\Omega} \cdot \mathbf{B} < 0$, and this binding depends on the ionic composition. We note the following three arguments for and against the composition being primarily ^{56}Fe.

(1) Rosen and Cameron (1972) showed that the outermost layers of the neutron star atmosphere, in which no mass is being ejected, are composed almost entirely of ^{4}He with trace amounts of ^{56}Fe. The ^{4}He is produced by photodissociation of the iron-peak nuclei (assumed to be the major initial constituent) at the high temperatures encountered during collapse to the neutron star state. The total mass of the ^{4}He at the neutron star surface is $\Delta M_{\rm He} \simeq 1{\cdot}3 \times 10^{18}\,{\rm kg} \sim 10^{-12} M_{\odot}$. However, the luminosity of a very young neutron star is highly super-Eddington, and so radiation pressure drives matter away from the neutron star surface. After the loss of about $10^{-12} M_{\odot}$, only ^{56}Fe remains at the surface (Rosen and Cameron 1972). For young neutron stars the mass-loss rate is as high as $\sim 0{\cdot}005\, M_{\odot}\,{\rm s}^{-1}$, and the mass ejected from the neutron star surface is of order 10^{-3}–$10^{-2} M_{\odot}$ (Woosley and Baron 1992; Levinson and Eichler 1993). Thus the ejected mass is $\gg \Delta M_{\rm He}$, suggesting that the neutron star surface consists almost entirely of ^{56}Fe.

(2) The composition of the polar caps of pulsars may differ substantially from the composition of the main part of the neutron star surface due to the bombardment by energetic particles from the magnetosphere. Pair particles created near the top edge of the polar gap and accelerated by the $E_{\|}$ field back to the stellar surface form showers as they cross the surface (Cheng and Ruderman 1977; Jones 1978, 1979). Protons and spallation nuclei are produced at the polar

caps of pulsars by hadronic photoabsorption of shower photons. The flux of reversed electrons (or positrons) through a unit surface area of the polar cap is

$$F_r = \xi n_{\rm GJ} c, \qquad (2\cdot2)$$

where ξ is a dimensionless parameter, with $\xi \sim 1$ for the model of Ruderman and Sutherland (1975) and $\xi \sim (\Omega R/c) \simeq 2 \times 10^{-3}(P/0{\cdot}1\,{\rm s})^{-1} \ll 1$ for the model of Arons (1979, 1981). The energy of reversed particles is $\Gamma_r mc^2$ with $\Gamma_r \sim 10^7$. Shower γ rays penetrate into the neutron star surface layers to $\sim$30 radiation lengths (Jones 1978; Bogovalov and Kotov 1989) and break up atomic nuclei. In the case of ^{56}Fe, for which the radiation length is $l_r \simeq 140\,{\rm kg\,m^{-2}}$, 30 radiation lengths corresponds to a column density $\sigma = 30 l_r \simeq 4{\cdot}2 \times 10^3\,{\rm kg\,m^{-2}}$. The mean number of photoabsorption events per one reversed particle with energy $\sim 10^7 mc^2$ is $\sim 10^3$ (Hayward 1965; Jones 1978). Hence, from equations (2·1) and (2·2), the characteristic time for spallation of all the ^{56}Fe in the surface layer, $\tau = (\sigma/Am_p)/10^3 F_r$ with $A = 56$, reduces to

$$\tau < (2\,{\rm s})\,\xi^{-1}\left(\frac{B_{\rm s}}{10^8\,{\rm T}}\right)^{-1}\left(\frac{P}{1\,{\rm s}}\right)(\cos\theta)^{-1}, \qquad (2\cdot3)$$

which is very much shorter than the age of any pulsar. This suggests that all the ^{56}Fe should be destroyed in the surface layers of the polar caps.

(3) There are several contrary arguments to the foregoing: (a) The most important photoabsorption reaction is the formation of the giant dipole resonance (e.g., Hayward 1965; Jones 1978), which, for iron-group nuclei, decays predominantly through neutron emission. Most of the photons with energies of $\sim$15–30 MeV mainly responsible for spallation of ^{56}Fe are generated in the deep layer, $\gtrsim 10\,l_r$, (e.g., Jones 1978; Bogovalov and Kotov 1989). This suggests that the surface layer itself is relatively unaffected by the bombardment. (b) The resulting neutrons are distributed more or less uniformly inside the surface layer due to diffusion (Jones 1978), and are recaptured by the other nuclei. Neutron capture can reform ^{56}Fe, so that it is not permanently destroyed. (c) If the magnetic field is strong enough, $B_{\rm s} > 5 \times 10^8$ T, so that solid magnetic metal is formed at the pulsar surface (see below), both the generation of photons with energies of $\sim$15–30 MeV and spallation of ^{56}Fe may be suppressed over a few l_r due to the Landau–Pomeranchuk effect (Rozental and Usov 1985), that is, due to the suppression of the formation of softer photons and pairs in the strong magnetic field. (d) For pulsars with $\boldsymbol{\Omega}\cdot\mathbf{B} < 0$ at the polar caps, so that ions are the particles ejected from the stellar surface, ejection of ions can dominate over spallation. If so, the spallation products are removed as fast as they are produced, and the surfaces of the polar caps consist mainly of ^{56}Fe.

In summary, the composition of the surface of the neutron star at its polar caps is uncertain. Below we let the mass number A of the surface ions be a free parameter, and for numerical estimates we assume it corresponds to ^{56}Fe.

2·3 Surface Structure of Neutron Stars with Strong Magnetic Fields

Whether an Arons-type or Ruderman–Sutherland-type model is relevant for the polar-cap region of the pulsar magnetosphere depends on whether or not

charged particles can escape freely from the surface of the neutron star due to thermionic emission. This in turn depends on (a) the binding energy, referred to here as the cohesive energy for ions and as the work function for electrons, and (b) the surface temperature. The cohesive energy, $\Delta\varepsilon_c$, was overestimated in earlier literature.

The structure of matter in the surface layers of neutron stars with $B_s \gg \alpha^2 B_{cr} \simeq 2{\cdot}35 \times 10^5\,\mathrm{T}$, where $\alpha = e^2/4\pi\varepsilon_0\hbar c = 1/137$ is the fine structure constant, is largely determined by the magnetic field (Ruderman 1971; cf. also Fushiki, Gudmundsson and Pethick 1989 and references therein). It has been suggested that the surfaces of magnetic neutron stars with $B_s \sim 10^8\,\mathrm{T}$ consist of a phase of matter where atoms form chains aligned along the field lines (Cheng, Ruderman and Sutherland 1974; Flowers *et al.* 1977). The density of the magnetic metal phase is

$$\rho_s \simeq (4 \times 10^6\,\mathrm{kg\,m^{-3}})\left(\frac{B}{10^8\,\mathrm{T}}\right)^{\frac{6}{5}}\left(\frac{A}{56}\right)\left(\frac{Z}{26}\right)^{-\frac{3}{5}}. \tag{2·4}$$

The cohesive energy of the condensed ^{56}Fe matter was estimated by Flowers *et al.* (1977), using a variational method, to be

$$\Delta\varepsilon_c \simeq (2{\cdot}6\,\mathrm{keV})\left(\frac{B}{10^8\,\mathrm{T}}\right)^{0{\cdot}7}. \tag{2·5}$$

The properties of both bulk matter and isolated atoms in strong magnetic fields have been reconsidered using various approaches, including variational methods (Müller 1984; Skjervold and Östgaard 1984*b*), the Thomas–Fermi and related methods (Skjervold and Östgaard 1984*a*), density functional methods (Jones 1985, 1986), the Hartree-Fock method (Neuhauser, Langanke and Koonin 1986; Neuhauser, Koonin and Langanke 1987), and the Thomas–Fermi–Dirac method with the Weizsäcker gradient correction (Abrahams and Shapiro 1991). These investigations imply that Flowers *et al.* (1977) overestimated the cohesive energy by a factor of at least a few. The most recent Thomas–Fermi–Dirac calculations with the Weizsäcker coefficient $\lambda = \frac{1}{9}$ (the TFD-$\frac{1}{9}$W method) gives the cohesive energy for ^{56}Fe to be $\Delta\varepsilon_c \simeq 0{\cdot}91\,\mathrm{keV}$ for $B = 10^8\,\mathrm{T}$, $\Delta\varepsilon_c \simeq 2{\cdot}9\,\mathrm{keV}$ for $B = 5 \times 10^8\,\mathrm{T}$, and $\Delta\varepsilon_c \simeq 4{\cdot}9\,\mathrm{keV}$ for $B = 10^9\,\mathrm{T}$ (Abrahams and Shapiro 1991). The results of these calculations may be approximated by

$$\Delta\varepsilon_c \simeq (0{\cdot}9\,\mathrm{keV})\left(\frac{B}{10^8\,\mathrm{T}}\right)^{0{\cdot}73}. \tag{2·6}$$

The errors introduced by the TFD-$\frac{1}{9}$W method are near one per cent of the binding energy of isolated atoms, which is (Abrahams and Shapiro 1991)

$$\varepsilon_b \simeq -(55\,\mathrm{keV})\left(\frac{Z}{26}\right)^{\frac{9}{5}}\left(\frac{B}{10^8\,\mathrm{T}}\right)^{\frac{2}{5}}. \tag{2·7}$$

From (2·6) and (2·7), it follows that at $B \sim 10^8\,\mathrm{T}$ the errors of the calculations, $\sim 10^{-2}\varepsilon_b$, are of the same order as the cohesive energy. Thus, the qualitative result of Flowers *et al.* (1977) that chains are energetically favoured over individual

atoms is questionable. It is worth noting that the value of $\lambda = \frac{1}{9}$ is the standard gradient expansion result for the nonmagnetic case (Lieb 1981 and references therein). If the value of λ for strong magnetic fields is smaller than $\frac{1}{9}$, the cohesive energy is smaller than that implied by (2·6). Moreover, if λ is small enough, free atoms are preferred over chains for $Z = 26$ at $B \lesssim$ a few $\times 10^8$ T (Neuhauser *et al.* 1986, 1987). Hence, at $B_s \lesssim$ a few $\times 10^8$ T there are two possibilities: either ^{56}Fe does not form a magnetic metal at the neutron star surface, or the surface is solid with a small cohesive energy per Fe atom, $\Delta\varepsilon_c < 2$–3 keV (Neuhauser *et al.* 1986). The existence of a magnetic metal is then unimportant for ejection of particles from the surface, as discussed below.

For $B > (0{\cdot}5\text{–}1) \times 10^9$ T the surface of a neutron star is probably a magnetic metal, provided that the surface temperature is smaller than the melting temperature, T_m. An estimate of T_m is (Slattery, Doolen and DeWitt 1980; Shapiro and Teukolsky 1983; Ogata and Ichimaru 1990)

$$T_m \simeq (5 \times 10^6\,\mathrm{K})\left(\frac{Z}{26}\right)^2\left(\frac{A}{56}\right)^{-\frac{1}{3}}\left(\frac{\rho}{10^7\,\mathrm{kg\,m^{-3}}}\right)^{\frac{1}{3}}, \tag{2·8}$$

where ρ, the density of the magnetic metal, may differ from ρ_s, as given by (2·4), by a factor two or so (Abrahams and Shapiro 1991). The cohesive energy in such a strong magnetic field may be more than 3–5 keV.

2·4 *Electron Ejection* ($\boldsymbol{\Omega} \cdot \mathbf{B} > 0$)

The flow of electrons away from the surface of a pulsar with $\boldsymbol{\Omega} \cdot \mathbf{B} > 0$, assuming the neutron star surface to be a magnetic metal, is determined either by thermionic emission or by field emission.

The important condition is that the current density, J_{th}, from thermionic emission provides the Goldreich–Julian charge density. The particles are quickly accelerated to relativistic energies above the surface, and hence this condition becomes

$$J_{th} > n_{\mathrm{GJ}} e c. \tag{2·9}$$

Screening due to this charge density then implies $E_\parallel = 0$ on the stellar surface.

For electrons, the current density due to thermionic emission is determined by the Richardson–Dushman equation (e.g., Gopal 1974):

$$J_{th} = \frac{em}{2\pi^2\hbar^3}(kT)^2 \exp\left(-\frac{w}{kT}\right), \tag{2·10}$$

where m is the electron mass, k is the Boltzmann constant and w is the work function of electrons. Typically, the value of w is near the Fermi energy, which is given for a magnetic metal by (Ruderman 1971; Flowers *et al.* 1977)

$$\varepsilon_{\mathrm{F}} = \frac{2\pi^4\hbar^4 Z^2\rho^2}{e^2 m_p^2 m A^2 B^2}. \tag{2·11}$$

From (2·4) and (2·11), we have

$$\varepsilon_{\rm F} \simeq (0{\cdot}8\,{\rm keV})\left(\frac{Z}{6}\right)^{\frac{4}{5}}\left(\frac{B}{10^8\,{\rm T}}\right)^{\frac{2}{5}}. \tag{2·12}$$

Taking $w \simeq \varepsilon_{\rm F}$ and using (2·2), (2·10) and (2·12), we can rewrite the condition (2·9) in terms of the characteristic temperature, T_e, identified as

$$T_e = 0{\cdot}04\frac{w}{k} \simeq (3{\cdot}7\times 10^5\,{\rm K})\left(\frac{Z}{26}\right)^{\frac{4}{5}}\left(\frac{B_{\rm s}}{10^8\,{\rm T}}\right)^{\frac{2}{5}}. \tag{2·13}$$

Then setting $T = T_{\rm s}$ as the surface temperature, (2·9) requires $T_{\rm s} > T_e$ for thermionic emission of electrons to be adequate to provide the Goldreich–Julian density.

Field emission is relevant only if thermionic emission is inadequate, that is, for $T_{\rm s} < T_e$. Then $E_\parallel$ is nonzero on the surface at the polar caps and the ejection of electrons results from quantum mechanical tunneling through the barrier provided by the work function and $E_\parallel$. The current density due to this tunneling is (Beskin 1982) $J = ME_\parallel \exp(-N/E_\parallel)$, $M = 3\times 10^{16}(B/10^8\,{\rm T})(w/1\,{\rm keV})^{-1/2}\,{\rm s}^{-1}$, $N = 2\times 10^{14}(w/1\,{\rm keV})^{\frac{3}{2}}\,{\rm V\,m}^{-1}$. Equating this to the current implied by an electron density $n_{\rm GJ}$ outflowing at the speed of light allows one to define a characteristic electric field:

$$E_e \simeq (6\times 10^{12}{\rm V\,m}^{-1})\left(\frac{w}{1\,{\rm keV}}\right)^{\frac{3}{2}}, \tag{2·14}$$

such that one requires $E_\parallel > E_e$ for field emission to be effective. For $E_\parallel \ll E_e$, the density of electrons ejected due to field emission is negligible. For $E_\parallel \gtrsim E_e$ the electrons escape freely until their density builds up to $\sim n_{\rm GJ}$, and they then screen the electric field, restricting it to $E_\parallel \sim E_e$.

2·5 Ion Ejection ($\boldsymbol{\Omega}\cdot\mathbf{B} < 0$)

The flow of ions away from the solid surface of a pulsar with $\boldsymbol{\Omega}\cdot\mathbf{B} < 0$ is limited by the rate of thermionic emission of ions. The density of outflowing ions is (Cheng and Ruderman 1980)

$$n_i \simeq n_{\rm GJ}\min(1,\zeta), \tag{2·15}$$

with

$$\zeta = \left(\frac{kT_{\rm s}}{1\,{\rm keV}}\right)^{\frac{1}{2}}\left(\frac{P}{1\,{\rm s}}\right)\left(\frac{B_{\rm s}}{10^8\,{\rm T}}\right)^{-1}\left(\frac{Z}{26}\right)\left(\frac{A}{56}\right)^{-\frac{3}{2}}\left(\frac{\rho_{\rm s}}{10^7\,{\rm kg\,m}^{-3}}\right)\exp\left(-\frac{30\Delta\varepsilon_c}{kT_{\rm s}}\right). \tag{2·16}$$

The value of n_i is very sensitive to the surface temperature for $T_{\rm s} \sim T_i$, where T_i is the characteristic temperature

$$T_i \simeq \frac{\Delta\varepsilon_c}{30\,k} \simeq (3{\cdot}5\times 10^5\,{\rm K})\left(\frac{B_{\rm s}}{10^8\,{\rm T}}\right)^{0{\cdot}73}, \tag{2·17}$$

and where the cohesive energy of the condensed ^{56}Fe matter in a strong magnetic field is estimated from (2·6). A small change in T_s around $T_s \sim T_i$ can have a large effect on n_i, with a change by a factor of two causing n_i/n_{GJ} to vary from exponentially small to approximately unity. For $T_s > T_i$ the existence of a magnetic metal at the neutron star surface does not affect the ejection of ions, and one has $E_\parallel = 0$ on the stellar surface.

Field emission of ^{56}Fe ions from a cold magnetic metal at the surface of pulsars with $B_s > 10^8$ T is unimportant for all known pulsars (Ginzburg and Usov 1972). Therefore, in the case $T_s < T_i$ there is no ejection of ions from the neutron star surface, and the electric field component $E_\parallel$ near the polar caps is nonzero and is determined by the polar-gap structure (e.g., Ruderman and Sutherland 1975 and below).

3. Particle Acceleration and Curvature Radiation

The acceleration of primary particles is due to the parallel electric field in the polar gaps. Curvature radiation is an important ingredient in the generation of the secondary pair plasma, and it can also limit the energy of the primary particles.

3·1 Particle Acceleration and Curvature Radiation

If the energy losses of a particle are neglected, then a primary particle ejected at the stellar surface reaches a maximum energy

$$\varepsilon = \Gamma mc^2 = e\Delta\varphi \qquad (3\cdot1)$$

at the top edge of the polar gap. Here Γ is the Lorentz factor and $\Delta\varphi$ is the potential across the polar gap.

In a strong magnetic field near the pulsar, electrons lose the momentum component transverse to the magnetic field very rapidly (timescale $\ll R/c$) and move away from the pulsar along the field lines. For such electrons in the ground-state Landau level, any energy loss is negligible up to the Lorentz factors of $\sim$10. For $10 \lesssim \Gamma \lesssim 10^2$, the energy loss due to cyclotron resonant scattering of thermal X-rays from the neutron star surface increases sharply and may be very important for both motion of electrons and their radiation (Dermer 1990 and references therein). At very high energies, $\Gamma \gg 10^3$–10^4, the main energy loss for ultrarelativistic electrons in the pulsar magnetospheres is due to curvature radiation. The rate of energy loss is (e.g., Ochelkov and Usov 1980)

$$|\dot{\varepsilon}| = \frac{e^2 c}{6\pi\varepsilon_0 R_c^2}\Gamma^4, \qquad (3\cdot2)$$

where R_c is the radius of curvature of the magnetic field lines. Equation (3·1) is valid only if the rate of energy loss, $|\dot{\varepsilon}|$, is smaller than the rate of energy gain, $eE_\parallel$, due to acceleration by the parallel electric field. The maximum energy of electrons cannot exceed the value implied by balancing these energy gains and losses, that is, the maximum is determined by $|\dot{\varepsilon}| \simeq eE_\parallel c$. The Lorentz factor of particles when this quasi-stationary state is achieved is

$$\Gamma \simeq \Gamma_{\rm st} = \left(\frac{6\pi\varepsilon_0 E_\parallel R_{\rm c}^2}{e}\right)^{\frac{1}{4}}. \tag{3·3}$$

Electrons in a strong magnetic field quickly radiate away their perpendicular momentum and are then in their lowest Landau level. Such electrons move along curved magnetic field lines and emit curvature radiation. The mean energy, $\bar{\varepsilon}_\gamma$, of curvature photons generated by ultrarelativistic electrons, $\Gamma \gg 1$, is

$$\bar{\varepsilon}_\Gamma = \tfrac{3}{2}\frac{\hbar c}{R_{\rm c}}\Gamma^3. \tag{3·4}$$

For $\Delta\varphi = \Delta\varphi_{\rm RS}$, $\Gamma = e\Delta\varphi_{\rm RS}/mc^2 \simeq 3 \times 10^6$ (Ruderman and Sutherland 1975) and $R_{\rm c} \simeq 10R \simeq 10^5\,{\rm m}$, from (3·4) we have $\bar{\varepsilon}_\gamma \simeq 10^2\,{\rm MeV}$. Thus the curvature radiation of electrons accelerated in the polar gaps falls in the γ-ray range. Note also that the mean energy satisfies $\bar{\varepsilon}_\gamma \gg 2mc^2 \simeq 1\,{\rm MeV}$.

3·2 Curvature γ rays and Pair Creation Threshold

A photon propagating in a strong magnetic field may decay into two photons or into pairs (Toll 1952; Klepikov 1954; Erber 1966; Adler 1971 and Section 4 below). Pair creation occurs only when the energy of the photons exceeds the threshold $\sim 2mc^2$ in the frame in which the photon is propagating perpendicular to the field lines (Section 4·2 below).

Although a particle in its lowest Landau level has no perpendicular motion in a uniform magnetic field, it does have a small perpendicular motion if the field lines are curved. The perpendicular motion is at the curvature drift velocity, $\mathbf{v}_c$, which is such that the Lorentz force, $\propto \mathbf{v}_c \times \mathbf{B}$, causes the particle to follow the curved field line (e.g., Zheleznyakov and Shaposhnikov 1979). The curvature drift implies a perpendicular momentum

$$p_{\rm cd} = \frac{p_\parallel^2}{m\omega_{\rm B} R_{\rm c}}, \tag{3·5}$$

where $\omega_{\rm B} = eB/mc$ is the gyration frequency. The angle, ψ, between the momentum vector $\mathbf{p}$ and the tangent to the magnetic field line, defined by $p_{\rm cd} = p\sin\psi$, $p_\parallel = p\cos\psi$, $p = |\mathbf{p}| = \Gamma mv$, is given by

$$\psi \simeq \frac{c\Gamma}{\omega_{\rm B} R_{\rm c}} \simeq 1{\cdot}7 \times 10^{-8}\left(\frac{B}{10^8\,{\rm T}}\right)^{-1}\left(\frac{\Gamma}{10^8}\right)\left(\frac{R_{\rm c}}{10^5\,{\rm m}}\right)^{-1}, \tag{3·6}$$

where (3·5) is used for $\psi \ll 1$.

A highly relativistic particle emits nearly all its radiation in a cone with half angle $\sim \Gamma^{-1} \ll 1$ about the momentum vector $\mathbf{p}$. Hence, the curvature photons are emitted in a cone nearly parallel to the field lines, but centred on an angle ψ away from the field lines. The question arises as to whether the condition for decay into pairs can be satisfied at the point of emission. The curvature photons have a perpendicular energy $\lesssim \bar{\varepsilon}_\gamma(\psi + \Gamma^{-1})$. Using (3·4) and (3·6), this energy is below the threshold ($2mc^2$) for pair creation for

$$\tfrac{3}{2}\frac{c\Gamma^2}{\omega_B R_c}\left(\frac{c\Gamma^2}{\omega_B R_c}+1\right) < \frac{2mc^2}{\hbar\omega_B}. \tag{3·7}$$

This condition corresponds to the Lorentz factor of ultrarelativistic particles being smaller than

$$\Gamma_* = \left\{\frac{R_c\omega_B}{c}\left[\left(\tfrac{1}{4}+\tfrac{4}{3}\frac{mc^2}{\hbar\omega_B}\right)^{\frac{1}{2}}-\tfrac{1}{2}\right]\right\}^{\frac{1}{2}}. \tag{3·8}$$

In the limits of a weak and strong magnetic field one gets

$$\Gamma_* \simeq \begin{cases} \left(\dfrac{4R_c^2 m\omega_B}{3\hbar}\right)^{\frac{1}{4}} & \text{for } B \ll B_{cr}, \\ \left(\dfrac{4R_c mc}{3\hbar}\right)^{\frac{1}{2}} & \text{for } B \gg B_{cr}, \end{cases} \tag{3·9}$$

which gives numerical values

$$\Gamma_* \simeq \left(\frac{R_c}{10^5\,\mathrm{m}}\right)^{\frac{1}{2}} \begin{cases} 2{\cdot}8\times 10^8\left(\dfrac{B}{10^8\,\mathrm{T}}\right)^{\frac{1}{4}} & \text{for } B \ll B_{cr}, \\ 5{\cdot}8\times 10^8 & \text{for } B \gg B_{cr}. \end{cases} \tag{3·10}$$

Inside the polar gap, the value of Γ is restricted by $\Gamma \lesssim \Gamma_{st}$, where Γ_{st} depends on $E_\parallel$, cf. (3·3). The upper limit on $E_\parallel$ when charged particles flow freely from the neutron star surface is (Arons 1981)

$$E_\parallel^{A} \simeq \frac{1}{8\sqrt{3}}\left(\frac{\Omega R}{c}\right)^{\frac{5}{2}} cB_s, \tag{3·11}$$

and when there is no particle flow from the surface the upper limit is (Ruderman and Sutherland 1975)

$$E_\parallel^{RS} \simeq \left(\frac{\Omega R}{c}\right)^{\frac{3}{2}} cB_s. \tag{3·12}$$

For all known pulsars one has $E_\parallel^{RS} \sim (10^2\text{–}10^4)\,E_\parallel^{A}$, implying $E_\parallel^{RS} \gg E_\parallel^{A}$.

Substituting $E_\parallel^{RS}$ into (3·3) and using (3·9) we have

$$\frac{\Gamma}{\Gamma_*} < \frac{\Gamma_{st}}{\Gamma_*} < 0{\cdot}2\left(\frac{P}{0{\cdot}1\,\mathrm{s}}\right)^{-\frac{3}{8}} \begin{cases} 1 & \text{for } B_s \ll B_{cr}, \\ \left(\dfrac{B_s}{B_{cr}}\right)^{\frac{1}{4}} & \text{for } B_s \gg B_{cr}. \end{cases} \tag{3·13}$$

From (3·13) it follows that Γ is smaller than Γ_* for all known pulsars except the millisecond pulsars. However, the magnetic field at the surface of millisecond pulsars, $B_s \sim 10^5$ T, is not strong enough to determine the structure of matter, and the magnetic metal phase does not form in the surface layers of the neutron

stars (Section 2). Therefore, particles flow freely from the surface of such a pulsar. In this case, $E_{\|}^{\mathrm{A}}$ is an upper limit on $E_{\|}$ in the pulsar magnetospheres. Substituting $E_{\|}^{\mathrm{A}}$ into (3·3) for $E_{\|}$ we get

$$\frac{\Gamma}{\Gamma_*} < \frac{\Gamma_{\mathrm{st}}}{\Gamma_*} < 2 \times 10^{-2} \left(\frac{P}{0{\cdot}1\,\mathrm{s}} \right)^{-\frac{5}{8}} . \tag{3·14}$$

Then the condition $P > 10^{-3}\,\mathrm{s}$, valid for all pulsars, in (3·14) implies $\Gamma < 0{\cdot}3\Gamma_*$ for the millisecond pulsars.

It follows that for all known pulsars the curvature photons generated near the neutron star surface are produced in a state below the pair creation threshold. In order to reach the threshold for decay into pairs (or the formation of positronium) the curvature photons must travel some distance, so that the angle between their wave vector and the magnetic field has increased sufficiently.

4. Propagation of γ Rays and Pair Creation

The propagation of γ rays in a strong magnetic field can lead both to splitting of one photon into two or more photons and to decay of a photon into a free or bound electron–positron pair. These processes can depend on which wave mode the photon is in.

4·1. Modes of Propagation for γ Rays

The conventional expression for the refractive index of a plasma, with the vacuum polarization by the magnetic field taken into account, differs from unity by the order of $[0{\cdot}1\alpha(B/B_{\mathrm{cr}})^2 + (\omega_p/\omega)^2]\sin^2\vartheta$, with $\omega_p = (e^2 n_p/\varepsilon_0 m)^{\frac{1}{2}}$, where n_p is the plasma density, $\omega = \varepsilon_\gamma/\hbar$ is the photon frequency and ϑ is the angle between the photon wave vector $\mathbf{K}$ and the magnetic field $\mathbf{B}$ (Erber 1966; Adler 1971; Shabad 1975). For $\omega \gg 3\alpha^{-1/2}(B_{\mathrm{cr}}/B)\omega_p$, the vacuum polarization gives the main contribution to the difference between the refractive index and unity. Near the pulsar surface, where $B \gtrsim 10^8\,\mathrm{T}$ and $n_p \lesssim 10^{26}\,\mathrm{m}^{-3}$ (Sturrock 1971; Ruderman and Sutherland 1975; Arons 1979, 1981, 1983), this condition becomes $\omega \gg 10^{18}\,\mathrm{s}^{-1}$, which is well satisfied for γ-quanta. Hence, to understand the process of γ-quantum propagation in the vicinity of a pulsar with $B_{\mathrm{s}} > 10^8\,\mathrm{T}$, it suffices to consider propagation in the vacuum polarized by a strong magnetic field.

The principal modes of propagation for a photon in the magnetized vacuum are linearly polarized with electric vectors either perpendicular ($\perp$ mode) or parallel ($\|$ mode) to the plane formed by the photon wave vector $\mathbf{K}$ and the vector $\mathbf{B}$. The labeling convention adopted here is standard, although other labelings of the the modes are used (e.g., Adler 1971; Usov and Shabad 1983). Both modes are generated in the process of the curvature radiation (Jackson 1975).

Photons in either mode can decay into a free electron–positron pair provided that a relevant threshold is exceeded (Toll 1952). For the $\|$ mode both the electron and the positron can be in their ground states, and the relevant threshold is

$$\varepsilon_\gamma \sin\vartheta = 2mc^2 . \tag{4·1}$$

For the $\perp$ mode the lowest allowed state requires that either the electron or the positron is in the first excited state, with the other in its ground state. The relevant threshold is then

$$\varepsilon_\gamma \sin\vartheta = mc^2\{1 + [1 + (2B/B_{\rm cr})]^{\frac{1}{2}}\}\,. \qquad (4\cdot2)$$

4·2 Curvature Photon Splitting in a Strong Magnetic Field

While the photon is below the pair creation threshold, its main (inelastic) interaction with the magnetic field is a splitting into two photons $\gamma + B \to \gamma' + \gamma'' + B$ (e.g., Adler *et al.* 1970; Bialynicka-Birula and Bialynicki-Birula 1970; Adler 1971; Stoneham 1979; Melrose 1983; Usov and Shabad 1983; Baring 1991 and references therein). For $B \lesssim B_{\rm cr}$, when radiative corrections are negligible, Bialynicka-Birula and Bialynicki-Birula (1970) showed that the splitting of a photon into more than two photons is unimportant. Adler (1971) showed that splitting involving an odd number of $\|$-polarized photons ($\|\to\| + \|$, $\|\to\perp + \perp$, $\perp\to\| + \perp$) is forbidden (by CP invariance), and that below the pair creation threshold, of the remaining transitions the only one that is kinematically allowed is $\perp\to\| + \|$. The probability for $\perp$-polarized photon splitting in the weak-field limit, $B \lesssim B_{\rm cr}$, is greatest when the energy of the initial photons is divided equally between the two final photons.

The optical depth τ_d for the splitting of $\perp$-polarized photons with $\varepsilon_\gamma \gg mc^2$ as they propagate from $\vartheta \simeq 0$ up to the pair creation threshold (4·2) is (Usov and Shabad 1983)

$$\tau_d \simeq 1{\cdot}7 \times 10^5 \left(\frac{B}{B_{\rm cr}}\right)^6 \left[1 + \left(1 + \frac{2B}{B_{\rm cr}}\right)^{\frac{1}{2}}\right]^7 \left(\frac{R_{\rm c}}{10^5\,{\rm m}}\right)\left(\frac{mc^2}{\varepsilon_\gamma}\right)^2 . \qquad (4\cdot3)$$

It follows from (4·3) that, if the strength of the magnetic field at the pulsar poles is high enough, $B_{\rm s} \gtrsim 10^9\,{\rm T}$, most of the $\perp$-polarized photons with $\varepsilon_\gamma \lesssim 10^2\,{\rm MeV}$ produced by curvature mechanism near the pulsar surface are split and transformed into the $\|$-polarized photons before the pair creation threshold is reached. However, the $\|$-polarized photons cannot be split below the pair creation threshold.

4·3 Bound Pair Production in a Strong Magnetic Field

If the photon energy is above the pair creation threshold, the main process by which a photon interacts with the magnetic field is single-photon absorption, accompanied by pair creation: $\gamma + B \to e^+ + e^- + B$ (Klepikov 1954; Erber 1966; Tsai and Erber 1974; Melrose and Parle 1983; Shabad and Usov 1984). In the application to pulsars it is usually assumed that the curvature γ-quanta produced below the pair creation threshold propagate as polarized photons through the pulsar magnetosphere until they are absorbed by creating free pairs. However, before a curvature photon reaches the threshold for free pair creation it must cross the threshold for bound pair creation (Usov and Shabad 1985; Shabad and Usov 1985, 1986, cf. also Pavlov and Mészáros 1993 and references therein). Hence, when considering the creation of free pairs by curvature photons in the strong magnetic fields of pulsars, the process of conversion into bound pairs, that is, into positronium atoms, needs to be considered.

4·3·1 Kinematic condition for positronium production. To specify the positronium state created by a photon with a given momentum $\hbar\mathbf{K}$, we choose a set of quantum numbers suggested by the special choice of gauge with

scalar potential zero and vector potential with components $A_x = -By$, $A_y = A_z = 0$ for the constant and homogeneous magnetic field $B = B_z$, $B_x = B_y = 0$. Since $\mathbf{A}$ does not depend on x, z or t, the x- and z-components of momentum and the energy are constants of the motion. Without loss of generality we choose the x-axis along $\hbar\mathbf{K}_\perp$. Conservation of the z-component of momentum implies that the parallel momentum of the centre of mass of the positronium is equal to the parallel component of the photon momentum: $\hbar K_\parallel = P_z = p_z^+ + p_z^-$, where $p_z^\pm$ are the parallel momentum components of the electron and positron.

For present purposes it suffices to consider the case $B \gg \alpha^2 B_{\rm cr} \simeq 2{\cdot}35 \times 10^5\,{\rm T}$, in which the orbital radius of the electron, $r_{\rm B} = (\hbar/eB)^{\frac{1}{2}}$, is much less than the Bohr radius, $a = 4\pi\varepsilon_0\hbar^2/me^2$. In this case the dependence of the electron and positron wave functions on the perpendicular motion is of the same form as when they do not form positronium (Schiff and Snyder 1939). The perpendicular motions of the electron and positron are then each described by a continuous and a discrete quantum number. The continuous quantum numbers, $p_x^\pm$, are interpreted as the y-coordinates of the gyrocentres $y^\pm$ through

$$y^\pm = \mp p^\pm/eB\,. \tag{4·4}$$

Conservation of the x-component of momentum then implies $\hbar K_\perp = P_x = p_x^+ + p_x^-$. Thus, a photon with perpendicular momentum component $\hbar K_\perp$ produces an electron and a positron whose gyrocentres are separated along the y-axis by $\hbar K_\perp/eB$. The Coulomb interaction between the electron and the positron affects only the wave functions of the relative motion along the magnetic field, and reduces to the problem of the one-dimensional hydrogen atom (Loudon 1959).

Thus, in a strong magnetic field the energy states of positronium in its rest frame may be labeled by five quantum numbers: $n \geq 0$ and $n' \geq 0$ for the Landau levels of the electron and positron, $n_c \geq 0$ for the principal quantum number of the one-dimensional hydrogen-like atom, the parity of the hydrogen-like atom state, and $P_x^2 \geq 0$ for the separation of gyrocentres of the electron and positron. The energy of positronium does not depend on $P_x^c = p_x^+ - p_x^-$, reflecting the fact that the energy cannot depend on the location of the centre of mass of the positronium in a uniform magnetic field.

The corrections to the dispersion relation for the two modes due to the polarization of the vacuum are not important in the present context. Hence we may approximate the dispersion relations, expressed as the energy of a photon, by the vacuum relation

$$\varepsilon_\gamma = \hbar c(K_\parallel^2 + K_\perp^2)^{\frac{1}{2}}\,. \tag{4·5}$$

The energy of positronium may be written

$$\varepsilon_p = \left[P_z^2c^2 + \varepsilon_{nn'}^2(n_c, P_x^2\hbar^{-2})\right]^{\frac{1}{2}}, \tag{4·6}$$

where

$$\varepsilon_{nn'}(n_c, P_x^2\hbar^{-2}) = mc^2\left[\left(1+\frac{2nB}{B_{\rm cr}}\right)^{\frac{1}{2}}+\left(1+\frac{2n'B}{B_{\rm cr}}\right)^{\frac{1}{2}}\right]-\Delta\varepsilon_{nn'}(n_c, P_x^2\hbar^{-2}) \tag{4·7}$$

is the rest energy of the positronium, with $\Delta\varepsilon_{nn'}(n_c, P_x^2\hbar^{-2})$ its binding energy.

Using both momentum conservation, $\hbar K_\perp = P_x$ and $\hbar K_\parallel = P_z$, and energy conservation, $\varepsilon_\gamma = \varepsilon_p$, we obtain the kinematic condition for positronium production by a photon in the form of an equation for $K_\perp$:

$$K_\perp = \frac{1}{c\hbar}\varepsilon_{nn'}(n_c, K_\perp^2)\,. \tag{4·8}$$

In order to establish whether this equation admits any solutions, one should know the positronium dispersion law, that is, the energy dependence on P_x. Unlike the case of free pair production by a photon in a magnetic field, to find the kinematic condition for bound pair production a dynamic problem has to be solved. This problem was considered by Shabad and Usov (1986) in detail, and the energy of a positronium atom was calculated for a state when all quantum numbers, n, n', n_c, P_z, P_x and $P_x^c = p_x^+ - p_x^-$, are arbitrary. Here the quantum number $P_x^c = -eB(y^+ + y^-)$ describes the location of the centre of mass of the positronium in the y-direction, cf. (4·4).

4·3·2 Energy of positronium and mixed photon–positronium states. When the two photon dispersion curves (identical curves for each mode) and the energy relations for positronium for each of the discrete states are plotted in momentum space, the intersection points between the curves define parameters where the photon and positronium states interact. The interaction may be described in terms of the dispersion curves for the photons and the energy curves for the positronium states reconnecting to form a set of mixed states. Each of these mixed states is photon-like in one limit and positronium-like in another limit. A kinematic restriction implies that photons in the two different modes can interact only with a positronium state of the appropriate parity. Hence, there are actually two distinct sets of mixed states, each applying only to one photon mode and one parity state of the positronium. An adiabatic change, corresponding to evolution along the dispersion curve, then allows a photon in one mode to evolve into positronium in the appropriate parity state.

Consider the simplest example, which is the ground state of the positronium, whose parity is positive and which interacts only with the $\parallel$ mode. For the ground state, $n = n' = n_c = 0$, the binding energy is (Shabad and Usov 1986)

$$\Delta\varepsilon_{00}(0,\, P_x^2\hbar^{-2}) = \alpha^2 mc^2\left[\ln\frac{a}{r_{\rm B}(1+r_{\rm B}^2P_x^2\hbar^{-2})^{\frac{1}{2}}}\right]^2. \tag{4·9}$$

Note that (4·9) applies only for $P_x \ll \hbar a/r_{\rm B}^2$, that is, for P_x such that the logarithm in (4·9) is positive. (This corresponds to the mean separation of the electron along the y axis being smaller than the Bohr radius.) The binding energy is small and positive for larger vaues of P_x, and it tends asymptotically

to zero as P_x^2 tends to infinity. Hence, if the magnetic field is strong enough, $B \gg \alpha^2 B_{\rm cr}$, the positronium energy ε_{00} varies in a narrow range from

$$\varepsilon_{00}(0,0) = mc^2\{2 - \alpha^2[\ln(a/r_{\rm B})]^2\}\,, \tag{4·10}$$

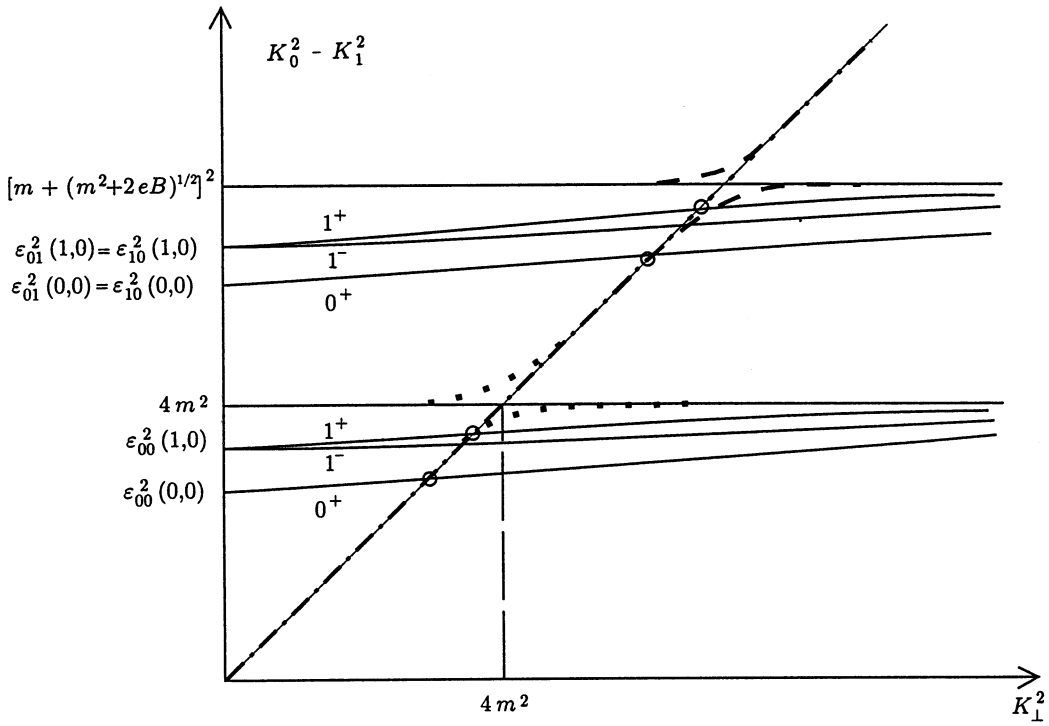

Fig. 1. Dispersion curves for photons, (4·5), and positronium, (4·6), are shown in the absence of interaction between them. The interactions occur near the relevant intersection points (circles). The positronium states, defined by (4·7) with $P_x = \hbar K_\perp$, are labelled with the quantum number n_c, and the parity under reflection along the z-axis (superscript). The only states shown are for $n_c = 0$ and 1 for the electron and positron in their lowest Landau orbital with antiparallel spins (lower set) and parallel spins (upper set). The modifications to the photon dispersion (oblique line) due to resonances in the vacuum polarization tensor are shown for ||-polarized (dotted curves) and ⊥-polarized (dashed curves) photons. [After Shabad and Usov 1986.]

to $2mc^2$ when P_x^2 varies from zero to infinity. Therefore, (4·8) must have a solution. It follows that positronium production by a photon in the || mode becomes kinematically allowed before the threshold of free pair production (4·1) is reached. A similar situation applies to a photon in the ⊥ mode near the second threshold of pair creation (Shabad and Usov 1986). Fig. 1 solves (4·8) graphically for both ||-polarized and ⊥-polarized photons.

When the photon and positronium dispersion curves are treated as independent, they are given by the following equations (Fig. 1):

$$\left(\frac{\varepsilon_\gamma}{\hbar c}\right)^2 - K_\parallel^2 = K_\perp^2\,, \tag{4·11}$$

for the photon, and

$$\left(\frac{\varepsilon_p}{\hbar c}\right)^2 - K_\parallel^2 = \left(\frac{mc}{\hbar}\right)^2 \left\{2 - \alpha^2 \left[\ln \frac{a}{r_B(1 + r_B^2 K_\perp^2)^{\frac{1}{2}}}\right]^2\right\}^2 \qquad (4\cdot12)$$

for the positronium with $n = n' = n_c = 0$. In (4·12) the parallel and perpendicular wave vectors, $K_\parallel = P_z\hbar^{-1}$ and $K_\perp = P_x\hbar^{-1}$, are used instead of P_z and P_x to describe the positronium state. Mutual transformations of the photon and positronium are kinematically allowed at the point satisfying $K_\perp = (K_\perp)_0$,

$$(K_\perp)_0 \simeq \frac{mc}{\hbar}\left\{4 - \alpha^2\left(\ln \frac{a}{r_B[1 + (4B_{cr}/B)]^{\frac{1}{2}}}\right)^2\right\}^{\frac{1}{2}}, \qquad (4\cdot13)$$

where, in the absence of any interference, the photon and positronium dispersion curves would intersect.

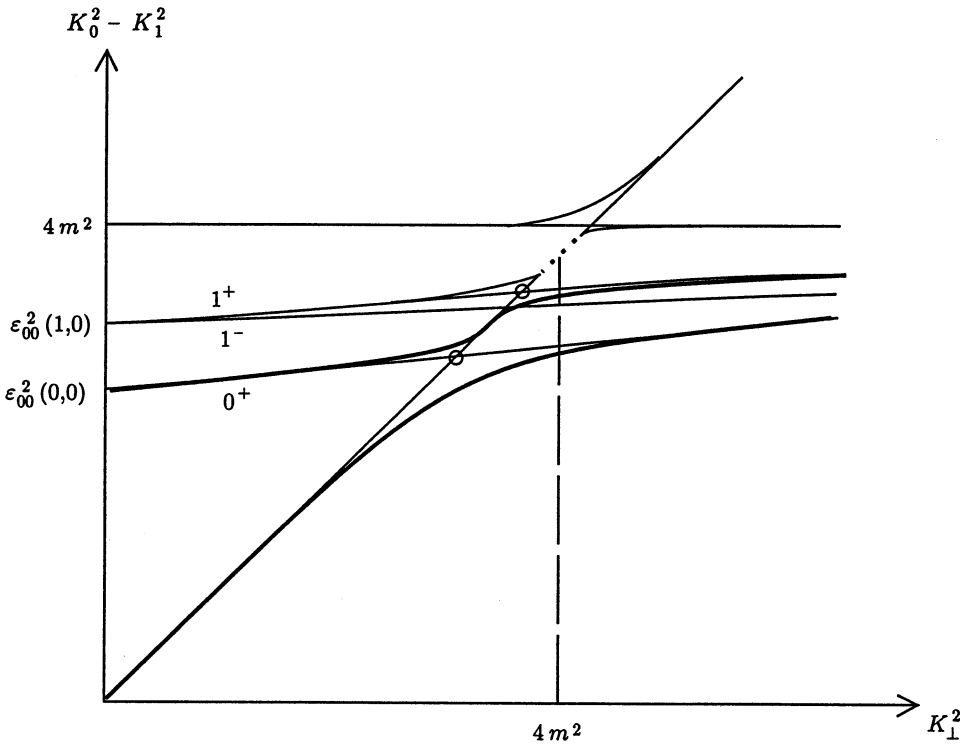

Fig. 2. As in Fig. 1, with the solid lines denoting the mixed (||-polarization/positive-parity) photon-positronium states. The dots denote higher order (in n_c) states that merge into a continuum near $\varepsilon = mc^2$. [After Shabad and Usov 1986.]

The dispersion curves of the photon and the positronium interfere strongly near $K_\perp^2 = (K_\perp)_0^2$. The dispersion curves repulse each other and reconnect to form mixed states (Fig. 2). This effect is quite general (Von Neumann and Wigner 1964) and is sometimes called the theorem on nonintersection of spectral terms.

For $n = n' = n_c = 0$, the split dispersion curves of the mixed states are (Shabad and Usov 1985, 1986)

$$\left(\frac{\varepsilon}{\hbar c}\right)^2 - K_\parallel^2 = \tfrac{1}{2}\left(\left[\frac{\varepsilon_{00}(0, K_\perp^2)}{\hbar c}\right]^2 + K_\perp^2 \pm \left\{\left[\left(\frac{\varepsilon_{00}(0, K_\perp^2)}{\hbar c}\right)^2 - K_\perp^2\right]^2 + 4A(K_\perp^2)\right\}^{\frac{1}{2}}\right), \quad (4\cdot14)$$

with

$$A(K_\perp^2) = \frac{4\alpha e B \varepsilon_{00}(0, K_\perp^2)}{\hbar^2 c^2 a} \ln\left[\frac{a}{r_B(1 + r_B^2 K_\perp^2)^{\frac{1}{2}}}\right] \exp\left(-\frac{\hbar K_\perp^2}{2eB}\right). \quad (4\cdot15)$$

The lower of the two dispersion curves (the minus sign in (4·14)) is photon-like for $K_\perp^2 \ll (K_\perp)_0^2$, and positronium-like for $K_\perp^2 \gg (K_\perp)_0^2$ (Fig. 2). The upper branch in Fig. 2 is positronium-like for $K_\perp^2 \ll (K_\perp)_0^2$. This upper branch crosses the dispersion curve of the odd state of the positronium with $n_c = 1$ without interfering with it (Shabad and Usov 1986). As $K_\perp^2$ grows further, the upper branch approaches the even positronium state with $n_c = 1$. There is an infinite set of bound positronium states at higher quantum numbers, and hence an infinite number of branches of the mixed-state dispersion curves below the limit, $(\varepsilon/\hbar c)^2 - K_\parallel^2 = (2mc/\hbar)^2$, that separates the bound states from the continuum of unbound electron–positron states.

4·3·3 Channelling along the magnetic field lines. A curvature photon is emitted almost parallel to the magnetic field below the pair creation threshold, $K_\perp^2 \ll (2mc/\hbar)^2$ (Section 3·3). Provided that the geometrical optics or adiabatic approximation applies, the curvature of the magnetic field lines causes the photon to shift along the lower branch of the dispersion curves in Fig. 2. As a result it passes through the mixed photon–positronium state and gradually turns into positronium when the condition

$$K_\perp^2 > (2mc^2/\hbar)^2 + \Delta K_\perp^2 \quad (4\cdot16)$$

is satisfied, where

$$\Delta K_\perp^2 = 2\left[A(2mc/\hbar)^2\right]^{\frac{1}{2}} = 4\alpha\left(\frac{mc}{\hbar}\right)^2 \left\{\frac{2B}{B_{cr}} \ln\frac{a}{r_B[1 + (4B_{cr}/B)]^{\frac{1}{2}}}\right\}^{\frac{1}{2}} \exp\left(-\frac{B_{cr}}{B}\right) \quad (4\cdot17)$$

is a measure of the gap between the lower and upper branches.

In order for γ-quantum absorption to lead to the formation of bound pairs rather than free pairs, the adiabatic approximation must apply. This requires that the time (Shabad and Usov 1986)

$$\tau_c \simeq \frac{\varepsilon_\gamma}{4mc^2} \frac{\Delta K_\perp^2}{K_\parallel^2} \frac{R_c}{c} \quad (4\cdot18)$$

needed to convert from the photon-dominated into positronium-dominated state should be much longer than the inverse frequency of the photon, $\omega^{-1} = \hbar/\varepsilon_\gamma$. For

photon energies $\varepsilon_\gamma \gg 2mc^2$ which are of interest here, we have $K_\parallel^2 \simeq (\varepsilon_\gamma/\hbar c)^2$. Taking this into account and using (4·15)–(4·17), the condition for the adiabatic approximation to apply, $\tau_c \gg \omega^{-1}$, can be written as a restriction on the magnetic field:

$$\left[\frac{2B}{B_{\rm cr}} \ln \frac{a}{r_{\rm B}[1+(4B_{\rm cr}/B)]^{\frac{1}{2}}}\right]^{\frac{1}{2}} \exp\left(-\frac{B_{\rm cr}}{B}\right) \gg \frac{a}{R_{\rm c}}. \tag{4·19}$$

For $R_{\rm c} \sim 10R \simeq 10^5$ m, (4·19) yields $B > 0{\cdot}03\,B_{\rm cr}$.

Another restriction is imposed by a widening of the dispersion curves that occurs because of the finite lifetimes of all excited states. In the case of the ∥-polarized photons, for kinematic reasons the state described by the lower dispersion curve of equation (4·14) cannot decay into two photons (cf. Section 4·2 and references therein). However, the positronium-dominated state which is described by the left part of the upper dispersion curve of equation (4·14), may decay into two photons. The probability of a two-photon positronium annihilation in a strong magnetic field ($B \sim 10^8$–10^9 T) is (Wunner and Herold 1979)

$$W_{2\gamma} \simeq (8 \times 10^{12}\,{\rm s}^{-1})\left(\frac{B}{10^8\,{\rm T}}\right), \tag{4·20}$$

for the case $K_\perp = 0$ in the positronium rest frame. The value of $W_{2\gamma}$ decreases as $K_\perp$ increases, so that (4·20) gives the maximum value of $W_{2\gamma}$.

The widening of the dispersion curves can be neglected if the energy gap between the ± branches is much larger than this widening. From (4·14), in the rest frame of the photon–positronium state, $K_\parallel = 0$, the energy gap is (Shabad and Usov 1986)

$$\Delta\varepsilon_g \simeq \hbar^2 \Delta K_\perp^2/4m. \tag{4·21}$$

The widening may be neglected in evaluating $\hbar W_{2\gamma}$. The field which gives $\Delta\varepsilon_g/\hbar W_{2\gamma} = 1$ may be found from (4·17), (4·20) and (4·21) to be about $0{\cdot}08\,B_{\rm cr}$. The ratio $\Delta\varepsilon_g/\hbar W_{2\gamma}$ is sensitive to the strength of the magnetic field: it is $\sim 10^{-4}$ for $B = 0{\cdot}05\,B_{\rm cr}$ and ~ 10 for $B = 0{\cdot}1\,B_{\rm cr}$. Hence, for $B \gtrsim 0{\cdot}1\,B_{\rm cr}$ the conditions for applicability of the dispersion curve (4·14) are fulfilled, and effectively all curvature γ-quanta in the ∥ mode are captured near the first threshold of bound pair creation by gradually converting into positronium. Positronium atoms with $n = n' = n_c = 0$ and $K_\perp^2 > (K_\perp)_0^2$ are stable against spontaneous decay into photons, which is forbidden by momentum and energy conservation (Herold *et al.* 1985; cf. also Adler 1971; Usov and Shabad 1983). Thus the positronium atoms formed by capture of the ∥-polarized photons in a strong magnetic field are stable, in the absence of such external factors as electric fields and ionizing radiation.

The ⊥-polarized photons cross the first threshold (4·1) without any pair creation, and pair creation is allowed only when the threshold (4·2) is reached. Positronium created by ⊥-polarized photons at this threshold have $n + n' \geq 1$, so that either the electron or the positron is in an excited state with the spin quantum number, $s = 1$, opposite to that in the ground state. In this case the main reason for the widening of the dispersion curve is a spin-flip transition, $s = 1 \to s = -1$. The probability of such a transition, W_s, has been

calculated for both the non-relativistic (Daugherty and Ventura 1978; Melrose and Zheleznyakov 1981) and the relativistic (Herold, Ruder and Wunner 1982) cases. The energy gap between the dispersion curves for a $\perp$-polarized photon mixed with the positronium state of the second series, $n = n_c = 0$, $n' = 1$ or $n' = n_c = 0$, $n = 1$, differs little from (4·21). The condition for bound pairs to dominate the absorption of $\perp$-polarized photons in a strong magnetic field is $\Delta\varepsilon_g > \hbar W_s$. Using the relativistic calculation of W_s (cf. Fig. 2 in Herold *et al.* 1982) and (4·21), we can write this condition as a restriction on the strength of the magnetic field: $B > 0{\cdot}15\,B_{\rm cr}$.

Summarizing, the main results of this section are as follows.

(1) For $B < 0{\cdot}04\,B_{\rm cr} \simeq 2 \times 10^8$ T, the creation of free electron–positron pairs dominates.

(2) For $0{\cdot}04\,B_{\rm cr} \lesssim B < 0{\cdot}1\,B_{\rm cr}$, the probabilities of creation of both positronium atoms and free pairs are more or less comparable and a numerical treatment is needed to determine the details.

(3) For $B \gtrsim 0{\cdot}1$–$0{\cdot}15\,B_{\rm cr}$ the curvature photons of both modes are captured near the pair creation thresholds.

Note that when the condition $B > 0{\cdot}15\,B_{\rm cr}$ is satisfied bound pair creation necessarily occurs. Bound pair creation occurs for lower values of B, and dominates over free pair creation for $B \gtrsim 0{\cdot}1\,B_{\rm cr}$.

4·4 Role of Strong Electric Fields

So far in our discussion of bound pair creation we have neglected the electric field in the pulsar magnetosphere. In general, both parallel, $\mathbf{E}_\parallel$, and perpendicular, $\mathbf{E}_\perp$, components are nonzero near the pulsar surface (Ruderman and Sutherland 1975; Arons 1979, 1981, 1983; Michel 1991). The field $\mathbf{E}_\perp$ causes a drift of particles across the magnetic field with velocity

$$\mathbf{v}_{\rm D} = \frac{\mathbf{E}_\perp \times \mathbf{B}}{B^2}, \tag{4·22}$$

provided one has $E_\perp < B$, a condition satisfied in the cases of interest here. In the pulsar magnetosphere at a point with radius vector $\mathbf{r}$, we may eliminate $\mathbf{E}_\perp$ by making a Lorentz transformation, with $\mathbf{v} = \mathbf{v}_{\rm D}(\mathbf{r})$, to the *drift frame*. Quantities in the drift frame are denoted by a tilde, so that we have $\tilde{\mathbf{E}}_\perp = 0$.

The characteristic time, $\tau_{\rm D}$, for a test particle to be dragged into motion across $\mathbf{B}$ with the mean velocity $\mathbf{v}_{\rm D}$ is of the order of the time of one gyration:

$$\tau_{\rm D} \simeq \omega_{\rm B}^{-1}\Gamma \simeq (10^{-12}\,{\rm s})\left(\frac{B}{0{\cdot}1\,B_{\rm cr}}\right)^{-1}\left(\frac{\Gamma}{10^8}\right). \tag{4·23}$$

For particles which are either ejected from the pulsar surface or created in the pulsar magnetosphere, the initial value of the Lorentz factor satisfies $\Gamma < \Gamma_{\rm st} \lesssim$ a few $\times 10^8$, cf. (3·3). As a consequence, the distance relativistic particles travel during the time $\tau_{\rm D}$ is much smaller than the characteristic scale of the electric field variation, of order the neutron star radius. Hence, particles acquire the drift motion very rapidly.

If the drift velocity $\mathbf{v}_D$ is nonuniform its effect cannot be removed entirely by a Lorentz transformation. Suppose the drift velocity varies along the field lines, so that the electric field $\tilde{E}_\perp$ changes with distance, z. Then, in addition to the curvature drift (3·6), the polarization drift contributes to the angle $\tilde{\psi}$ between the particle velocity $\tilde{\mathbf{v}}$ and the magnetic field $\tilde{\mathbf{B}}$ (Appendix A):

$$\tilde{\psi} \leq \frac{m\gamma}{eB^2}\frac{E_\perp}{\Delta l} \simeq 3{\cdot}8\times 10^{-8}\frac{E_\perp}{cB}\left(\frac{\Delta l}{10^4\,\mathrm{m}}\right)^{-1}\left(\frac{B}{0{\cdot}1\,B_{\mathrm{cr}}}\right)^{-1}\left(\frac{\Gamma}{10^8}\right), \quad (4{\cdot}24)$$

which applies to a particle in its lowest Landau level, and where Δl is a characteristic scale length of the electric field variation. Emission of curvature photons is centred on the direction of the velocity of the particle, which is at angle $\tilde{\psi}$. For these curvature photons to be produced below the pair creation threshold requires

$$\tilde{\varepsilon}_\gamma \sin\tilde{\psi} < 2mc^2\,. \quad (4{\cdot}25)$$

Assuming $\tilde{\Gamma} \simeq \Gamma$, $\tilde{\varepsilon}_\Gamma \simeq \varepsilon_\Gamma$, $\tilde{B} \simeq B$, $\Gamma < \Gamma_{\mathrm{st}}$, $E_\parallel \lesssim (E_\parallel^{\mathrm{RS}})_{\max}$ and $E_\perp/B \lesssim \Omega R$, and using (3·3), (3·4), (3·12) and (4·24), condition (4·25) gives

$$\frac{9\pi\varepsilon_0 c\hbar}{2e^2}\left(\frac{\Omega R}{c}\right)^{\frac{5}{2}}\frac{R_c}{\Delta l} < 1 \quad (4{\cdot}26)$$

or

$$P > (1{\cdot}6\times 10^{-3}\,\mathrm{s})\left(\frac{R_c}{\Delta l}\right)^{\frac{2}{5}}. \quad (4{\cdot}27)$$

For $\Delta l \sim R_c$ near the neutron star surface, (4·27) is fulfilled for most pulsars with the only exceptions being a few millisecond pulsars. However, as mentioned above, the strength of the magnetic field at the surface of known millisecond pulsars is $\sim 10^5$ T, that is, much smaller than $0{\cdot}1\,B_{\mathrm{cr}}$. For all known pulsars with strong magnetic fields, $B_s \gtrsim 0{\cdot}1\,B_{\mathrm{cr}}$, we have $P \gg 10^{-3}$ s, and hence the curvature photons generated near their surface are produced in a state below the pair creation threshold irrespective of existence of the field $E_\perp$ in the pulsar magnetosphere. Provided that the energy of the curvature photon is high enough, $\varepsilon_\gamma \gg 2mc^2$, as the photon propagates it approaches the threshold for pair creation. With the characteristic scale of variation of the field $E_\perp$ many orders of magnitude larger than the size of positronium atoms, at any instant we can introduce the frame with $\mathbf{E}_\perp = 0$. In this frame our consideration of bound pair creation is applicable, implying that bound pairs must be created by the curvature photons for $B > 0{\cdot}1\,B_{\mathrm{cr}}$.

The parallel electric field can lead to *field ionization* of the positronium. The Coulomb field and $E_\parallel$ combine to form a potential barrier, and quantum mechanical tunneling through this barrier leads to a nonzero probability for the decay of the bound state into a free electron and a free positron (Herold *et al.* 1985; Shabad and Usov 1985; Bhatia *et al.* 1988). The probability of the field ionization in the rest frame of the positronium is (Shabad and Usov 1985)

$$W_{\rm E} = \frac{eE_{\parallel}}{2\sqrt{m}\,(\Delta\varepsilon_{00})^{\frac{1}{2}}} \exp\left[\frac{-4\sqrt{m}\,(\Delta\varepsilon_{00})^{\frac{3}{2}}}{3e\hbar E_{\parallel}}\right]. \tag{4·28}$$

The value of $W_{\rm E}$ is very sensitive to the field $E_{\parallel}$. Provided that the strength of the field $E_{\parallel}$ near the pulsar is less than

$$E_{\parallel}^{\rm ion} \simeq \tfrac{2}{3}\frac{\sqrt{m}\,(\Delta\varepsilon_{00})^{\frac{3}{2}}}{e\hbar}\left(\ln\frac{R\,\Delta\varepsilon_{00}}{c\hbar\Gamma}\right)^{-1}, \tag{4·29}$$

the ionization probability of the positronium before it escapes from the pulsar environment is negligible. For $E_{\parallel} \gtrsim 2E_{\parallel}^{\rm ion}$, the mean free path of positronium atoms is much smaller than the neutron star radius, and positronium atoms are ionized almost immediately after their formation. Moreover, if the field $E_{\parallel}$ is so strong that the characteristic time of the positronium ionization, $(W_{\rm E})^{-1}$, is of the order of or smaller than the characteristic time of the photon conversion, τ_c, into a bound pair, cf. (4·18) and (4·28), then free electron–positron pairs rather than bound pairs are created by the curvature photons.

Numerically, $E_{\parallel}^{\rm ion}$ varies slowly with the magnetic field and with the Lorentz factor of the positronium. For $B_{\rm s} \simeq (0{\cdot}1\text{–}1)B_{\rm cr}$ and $\Gamma \sim 10\text{–}10^6$, (4·29) gives $E_{\parallel}^{\rm ion} \simeq 10^{12}\,{\rm V\,m^{-1}}$ to within a factor of 2 or so.

4·5 Photoionization of Positronium Atoms

Positronium atoms can be destroyed through ionization by photons. The main source of such photons is thermal radiation from the neutron star surface. The surface temperature of neutron stars, with ages $\sim 10^3\text{–}10^6$ yr, is usually estimated to be $\sim 10^5\text{–}10^6\,{\rm K}$ (e.g., Van Riper 1991; Page and Applegate 1992 and references therein) These estimates are more or less in agreement with recent observations of X-rays from a few pulsars. The mean free path for relativistic positronium, $\Gamma \gg 1$, against photoionization is

$$l_{\rm ph} \simeq c\Gamma(W_{\rm ph})^{-1}, \tag{4·30}$$

where $W_{\rm ph}$ is the probability of the positronium photoionization in the rest frame.

The value of $W_{\rm ph}$ was calculated numerically by Bhatia *et al.* (1992) for $B = 4{\cdot}7 \times 10^8\,{\rm T}$ and $K_{\perp} = (K_{\perp})_0 \simeq 2mc/\hbar$. The results of their calculations may be approximated by the analytic expression

$$W_{\rm ph} \simeq (6 \times 10^7\,{\rm s^{-1}})\left(\frac{\Gamma}{10^2}\right)^{-2}\left(\frac{T_{\rm s}}{10^6\,{\rm K}}\right)^{2}, \tag{4·31}$$

which is valid for $10^2 \le \Gamma \le 10^4$ and $10^5 \le T_{\rm s} \le 10^6\,{\rm K}$ with the accuracy ~20%. Equations (4·30) and (4·31) yield

$$l_{\rm ph} \simeq (0{\cdot}5 \times 10^3\,{\rm m})\left(\frac{\Gamma}{10^2}\right)^{3}\left(\frac{T_{\rm s}}{10^6\,{\rm K}}\right)^{-2}. \tag{4·32}$$

Note that only photons with energy $\varepsilon_\gamma \simeq (1\text{–}3)\Delta\varepsilon_{00}$ in the rest frame contribute to the decay of the positronium (Bhatia *et al.* 1992). Hence, the dependence of $W_{\rm ph}$ on B and $K_\perp$ is through the B and $K_\perp$ dependence of the binding energy, which may be written in the form, cf. (4·9),

$$\Delta\varepsilon_{00}(0, K_\perp^2, B) \simeq \frac{\alpha}{4} mc^2 \left[\ln \frac{B}{\alpha^2 B_{\rm cr}} \left(1 + \frac{4B_{\rm cr}}{B} \frac{K_\perp^2}{(2mc/\hbar)^2} \right)^{-1} \right]^2 . \quad (4\cdot33)$$

From (4·33) we infer that the B and $K_\perp$ dependence of $W_{\rm ph}$ is only logarithmic, and hence (4·32) may be used to estimate the order of $l_{\rm ph}$ for $0\cdot1\,B_{\rm cr} \lesssim B \lesssim B_{\rm cr}$ and $K_\perp \gtrsim 2mc/\hbar$.

5. Polar Gaps and Nonthermal Luminosities of Pulsars

As discussed in Section 4, adiabatic conversion of the curvature γ-quanta into mutually bound pairs in a strong magnetic field may result in these pairs not screening the electric field near the pulsar. The potential $\Delta\varphi$ across the polar gaps may then exceed $\Delta\varphi_{\rm RS}$, leading to an increase in the theoretical estimate of the total energy flux carried by relativistic particles from the polar gaps into the pulsar magnetosphere. In this section we explore how polar-gap models need to be modified to apply to pulsars with strong magnetic fields to take account of the role played by bound pairs. Assuming free ejections from the stellar surface, we find that the modification gives at most a modest enhancement in the energy flux in primary particles, and this is inadequate to account for the observed nonthermal emission from some pulsars. Alternatively, assuming limited ejection from the stellar surface, we argue that there is a feedback mechanism that favours a self-consistent model. The energy flux in primary particles in this model appears capable of accounting for the observed nonthermal emission from most of the observed high-frequency pulsars.

5·1 Free Ejection of Electrons from the Polar Cap

First consider the case where electrons flow freely from the surface of the neutron star, which occurs when the temperature of the polar caps satisfies $T_{\rm s} > T_e$, cf. (2·13). The model of Arons is then assumed to apply, with $E_\parallel = 0$ at the stellar surface. In the outflowing plasma at distance r from the centre of the neutron star, $E_\parallel$ may be as high as (Arons and Scharlemann 1979)

$$E_\parallel \simeq E_\parallel^{\rm A} \sin i \times \begin{cases} s/\Delta R_p & \text{at} \quad 0 \le s < \Delta R_p, \\ (R/r)^{\frac{1}{2}} & \text{at} \quad s > \Delta R_p, \end{cases} \quad (5\cdot1)$$

where i is the angle between the stellar magnetic moment and the spin axis, $s = r - R$ is the distance from the surface of the star, $\Delta R_p \simeq (\Omega R/c)^{\frac{1}{2}} R$ is the radius of the polar cap, $\Delta R_p \ll R$, and $E_\parallel^{\rm A}$ is given by (3·11). Here and below we consider a pulsar with a dipole magnetic field. The potential which corresponds to the electric field $E_\parallel$ is

$$\varphi(r) \simeq \frac{1}{8\sqrt{3}}\left(\frac{\Omega R}{c}\right)^{\frac{5}{2}} cB_{\rm s}\sin i \times \begin{cases} \dfrac{s^2}{2\Delta R_p} & \text{at } s \le \Delta R_p, \\ 2R\left[\left(\dfrac{r}{R}\right)^{\frac{1}{2}} - 1\right] - \dfrac{\Delta R_p}{2} & \text{at } s > \Delta R_p. \end{cases} \tag{5·2}$$

The total power carried away by both relativistic particles and radiation from the polar gap into the pulsar magnetosphere is

$$L_p \simeq \dot{N}_{\rm prim} e \Delta\varphi\,, \tag{5·3}$$

where $\dot{N}_{\rm prim}$ is the flux of primary electrons from the polar cap, $\Delta\varphi = \varphi(R+H) - \varphi(R)$ is the potential across the polar gap and H is the thickness of the polar gap. Equation (5·3) is valid irrespective of whether the pairs created near the pulsar are free or bound. The version of pair creation determines only the thickness of the polar gap, H, and thereby affects the value of L_p.

Assuming that the pairs created by the curvature photons are free, the thickness of the polar gap, $H = H_f$, is (Arons 1981, 1983)

$$H_f \simeq \begin{cases} (7\times 10^2\,{\rm m})\left(\dfrac{B_{\rm s}}{10^8\,{\rm T}}\right)^{-\frac{2}{5}}\left(\dfrac{P}{33\,{\rm ms}}\right)^{\frac{11}{20}}(\sin i)^{-\frac{3}{10}} & \text{at } P < P_d, \\ (1\times 10^4\,{\rm m})\left(\dfrac{B_{\rm s}}{10^8\,{\rm T}}\right)^{-1}\left(\dfrac{P}{0{\cdot}1\,{\rm s}}\right)^{\frac{17}{8}}(\sin i)^{-\frac{3}{4}} & \text{at } P > P_d\,, \end{cases} \tag{5·4}$$

where

$$P_d \simeq (0{\cdot}03\,{\rm s})\left(\frac{B_{\rm s}}{10^8\,{\rm T}}\right)^{\frac{8}{21}}(\sin i)^{\frac{2}{7}} \tag{5·5}$$

is the value of the pulsar period at which H is equal to ΔR_p.

The formation of bound rather than free pairs is important for $B_{\rm s} > 0{\cdot}1\,B_{\rm cr}$. Near the polar cap of the pulsar the condition $B > 0{\cdot}1\,B_{\rm cr}$ is satisfied up to a height

$$H_b = R\left[\left(\frac{B_{\rm s}}{0{\cdot}1\,B_{\rm cr}}\right)^{\frac{1}{3}} - 1\right] \tag{5·6}$$

above the pulsar surface. Thus, for $H_b > H_f$, bound pairs rather than free pairs are created in the polar gaps. In this case, provided that the probability of ionization of the bound pairs near the polar caps is sufficiently small, the thickness of the polar gaps could satisfy $H \sim H_b$. It follows that for $H_b > H_f$ one needs to consider the ionization of bound pairs near the polar caps inside the layer $0 \le s \le H_b$ when estimating the values of both H and $L_{\rm nth}^{\rm max}$.

For positronium atoms the probability of field ionization is negligible for $E_{\parallel}^{\rm A} < E_{\parallel}^{\rm ion} \simeq 10^{12}\,{\rm V\,m^{-1}}$ (Section 4·4). Using (3·11) this condition may be written in the form

$$P > (0{\cdot}8 \times 10^{-2}\,\mathrm{s})\left(\frac{B}{0{\cdot}1\,B_{\mathrm{cr}}}\right)^{\frac{2}{5}}, \tag{5·7}$$

which is satisfied for all known pulsars.

The mean free path for photoionization increases rapidly with increasing Lorentz factor of the bound pair, $l_{\mathrm{ph}} \propto \Gamma^3$, cf. (4·32). It follows that the photoionization of bound pairs with energy near the low-energy edge of their spectrum makes the main contribution to the density of free particles inside the polar gaps. This differs qualitatively from the case of $B < 0{\cdot}1\,B_{\mathrm{cr}}$ for which the high-energy tail of curvature photons is responsible for both the creation of free pairs in the polar gaps and the screening of the electric field $E_{\parallel}$ (Ruderman and Sutherland 1975; Arons 1981).

Let us estimate the height, H_i, above the stellar surface at which photoionization of bound pairs is efficient enough to determine the structure of the polar gaps. The lower limit on the Lorentz factor of pairs created at the distance s from the pulsar surface is (Appendix B)

$$\Gamma_{\mathrm{min}} = \tfrac{4}{3}\left(\frac{c}{\Omega R}\right)^{\frac{1}{2}}\frac{R}{s}. \tag{5·8}$$

The energy of the curvature photons responsible for the creation of pairs with the Lorentz factor Γ_{min}, $\hbar\omega = 2\Gamma_{\mathrm{min}}mc^2$, is less than the mean energy of the curvature photons radiated by the primary particles in the polar gaps, $\hbar\omega \ll (3\hbar c/2R_c)\Gamma^3$, where Γ is the Lorentz factor of primary particles accelerated in the polar gaps (Section 3·1). In this case the spectral power of curvature radiation does not depend on Γ and is given by (e.g., Ochelkov and Usov 1980)

$$p(\omega) \simeq \frac{e^2}{4\pi\varepsilon_0 c}\left(\frac{c}{R_c}\right)^{\frac{2}{3}}\omega^{\frac{1}{3}}. \tag{5·9}$$

At distance s from the pulsar surface the density of the curvature photons with energy $\hbar\omega = 2\Gamma_{\mathrm{min}}mc^2$ is

$$n_\gamma \simeq n_{\mathrm{GJ}}\frac{p(\omega)}{\hbar}\frac{s}{c}. \tag{5·10}$$

Taking into account the motion of the pair, the probability of photoionization of bound pairs in the frame of the pulsar is W_{ph}/Γ. From (4·31) and (5·8)–(5·10) we have the following estimate of the density of free pairs, $n_\pm$, created near the polar caps:

$$n_\pm \simeq n_\gamma\frac{W_{\mathrm{ph}}}{\Gamma_{\mathrm{min}}}\frac{s}{c}, \tag{5·11}$$

or

$$\frac{n_\pm}{n_{\mathrm{GJ}}} \simeq 1{\cdot}6 \times 10^6\left(\frac{P}{0{\cdot}1\,\mathrm{s}}\right)^{-\frac{4}{3}}\left(\frac{s}{R}\right)^{\frac{14}{3}}\left(\frac{T_{\mathrm{s}}}{10^6\,\mathrm{K}}\right)^2, \tag{5·12}$$

where we assume $R_c = 10^5$ m in (5·9). If at distance s the density of free pairs, $n_\pm$, exceeds about $n_{GJ}(\Omega R/c)$ (Arons 1981, 1983), the field $E_\parallel$ is screened at distances beyond s. This condition together with (5·12) gives a lower limit on the height, $H = H_i^{\min}$, for photoionization of bound pairs near the pulsar surface to be important:

$$H_i^{\min} \simeq (1{\cdot}3 \times 10^2 \text{ m}) \left(\frac{P}{0{\cdot}1 \text{ s}}\right)^{\frac{1}{14}} \left(\frac{T_s}{10^6 \text{ K}}\right)^{-\frac{3}{7}}. \tag{5·13}$$

In our estimate of the density of free pairs, $n_\pm$, cf. (5·12), the energy $2\gamma_{\min}mc^2$ is adopted for both the curvature photons and the created pairs. However, this energy is only the threshold for pair creation, and the actual mean energy may be a factor two or so higher. Alternative assumptions that give an estimate of the maximum value, $H = H_i^{\max}$, of H_i are that all curvature photons are generated by primary particles at $s = 0$, and all are emitted at threshold. If we assume that the mean energy of each pair is $4\Gamma_{\min}mc^2$, from (5·8) and (5·11) we have $s \simeq H_i^{\max} \simeq 3H_i^{\min}$. We assume $H_i = 2H_i^{\min}$.

Our estimate of the thickness of the polar gaps is (for $H_b > H_f$)

$$H = \min\{H_b, \max[H_f, H_i]\}. \tag{5·14}$$

In summary, for free electron ejection from the polar cap, any increase in $L_{\text{nth}}^{\max}$ is rather small for all known pulsars, and it cannot be accounted for with the strong nonthermal X-rays and γ-rays observed from a few pulsars. The main reason for this is that $E_\parallel$ in the outflowing plasma is rather weak, and the thickness, H_f, of the polar gaps is large even before taking into account its increase due to the creation of bound pairs. Hence, the potential $\Delta\varphi \sim E_\parallel H_f$ is modest and, with at best a modest increase in H, it is not possible to increase $\Delta\varphi$ substantially.

5·2 Limited Ejection of Electrons

Now consider the opposite case where electrons do not flow freely from the stellar surface. This requires that two conditions be satisfied simultaneously: thermionic emission of electrons must be ineffective, and ejection of electrons due to field emission must be ineffective. The former of these conditions requires $T_s < T_e$, cf. (2·13), and the latter requires $E_\parallel < E_e$, cf. (2·14). Provided these conditions are satisfied, $E_\parallel$ near the pulsar surface is of order the vacuum value $E_\parallel^{\text{RS}} \simeq (\Omega R/c)^{\frac{3}{2}} cB_s$, which is about $8\sqrt{3}(c/\Omega R) \sim 10^2$–$10^4$ times the maximum value of $E_\parallel$ in the Arons model, cf. (3·11).

Assuming that B is strong enough for the formation of bound pairs to occur, the pairs can play a significant role in modifying the model only if they remain bound within the polar gap. This requires $E_\parallel^{\text{ion}} < E_\parallel^{\text{RS}}$ within the polar gap. The conditions $E_\parallel^{\text{ion}} < E_\parallel^{\text{RS}}$ and $E_\parallel^{\text{RS}} < E_e$ can be satisfied only for $E_\parallel^{\text{ion}} < E_e$. For $B \simeq (0{\cdot}1\text{–}1)B_{\text{cr}}$, comparison of (2·14) and (4·29) with (4·33) shows $E_\parallel^{\text{ion}} \sim 0{\cdot}1\, E_e$,

implying that there can be a range, $E_{\parallel}^{\rm ion} < E_{\parallel}^{\rm RS} < E_e$, where escape from the surface is restricted and where field ionization of bound pairs is unimportant.

Assuming that there is no free ejection from the stellar surface and that bound pairs are not ionized, vacuum conditions apply, and hence the field $E_{\parallel}$ near the polar caps should be (Ruderman and Sutherland 1975):

$$E_{\parallel}(s,\rho) \simeq \frac{(\Delta R_p)^2 - \rho^2}{(\Delta R_p)^2} \exp\left(-\frac{2s}{\Delta R_p}\right) E_{\parallel}^{\rm RS}, \tag{5·15}$$

where ρ is the distance to the magnetic axis. Granted that $E_{\parallel}$ is unscreened, and so is given by (3·12), the condition $E_{\parallel}^{\rm RS} = E_{\parallel}^{\rm ion}$ defines a minimum period $P = P_1$ longer than which field ionization is unimportant:

$$P_1 = \frac{2\pi R}{c}\left(\frac{cB_{\rm s}}{E_{\parallel}^{\rm ion}}\right)^{\frac{2}{3}} \simeq (0{\cdot}5\,{\rm s})\left(\frac{R}{10^4\,{\rm m}}\right)\left(\frac{B_{\rm s}}{0{\cdot}1\,B_{\rm cr}}\right)^{\frac{2}{3}}. \tag{5·16}$$

In the following discussion we assume $P < P_1$, so that field ionization is important.

There is an inconsistency if one assumes either that $E_{\parallel}$ is much smaller or much larger than $E_{\parallel}^{\rm ion}$. On the one hand, suppose that ejection of electrons from the stellar surface is severely limited, implying $E_{\parallel} \simeq E_{\parallel}^{\rm RS} \gg E_{\parallel}^{\rm ion}$. For $P < P_1$ bound pairs created in the region $0 \le s < \frac{1}{2}\Delta R_p$ are ionized before they escape from this region. The resulting free positrons are accelerated toward the surface of the star, producing an intense flux that heats the polar cap. In the absence of ejection of electrons from the pulsar surface the temperature at the polar cap would be (Ruderman and Sutherland 1975)

$$T_{\rm RS} \simeq (10^7\,{\rm K})\left(\frac{B_{\rm s}}{0{\cdot}1\,B_{\rm cr}}\right)^{\frac{1}{14}}\left(\frac{P}{P_1}\right)^{-\frac{3}{14}}. \tag{5·17}$$

It follows from (2·13) and (5·17) that, for both $B_{\rm s} = (0{\cdot}1\text{–}1)B_{\rm cr}$ and $P < P_1$, $T_{\rm RS}$ is about an order of magnitude more than T_e, as given by (2·13). This implies that thermionic emission (due to the heating by positron bombardment) would produce an intense flux of electrons from the polar cap for temperatures well below $T_{\rm RS}$. This invalidates the original assumption that electron flow from the surface is severely limited. On the other hand, if one assumes $E_{\parallel} \ll E_{\parallel}^{\rm ion}$ for $P < P_1$, then field ionization of bound pairs is negligible, and both the heating of the polar caps by reversed particles and the screening of the field $E_{\parallel}$ are ineffective. As a result, one should have the vacuum field $E_{\parallel} = E_{\parallel}^{\rm RS}$, which invalidates the assumption $E_{\parallel} \ll E_{\parallel}^{\rm ion}$.

This inconsistency is avoided only if there is partial but not total screening of $E_{\parallel}$ inside the polar gap. Specifically, this field needs to be restricted to $E_{\parallel} \sim (1\text{–}2)E_{\parallel}^{\rm ion}$. This is possible through a feedback mechanism. To see that there is a feedback, suppose $E_{\parallel}$ decreases. This causes the rate of ionization of the bound pairs to decrease, so that the number of returning positrons heating the polar cap decreases, the temperature of the polar cap decreases and the rate of thermionic emission decreases. This leaves fewer (primary) electrons to screen $E_{\parallel}$, which increases toward $E_{\parallel}^{\rm RS}$, providing the feedback. An analogous argument leads to the conclusion that a postulated increase in $E_{\parallel}$ implies a sequence of processes causing $E_{\parallel}$ to decrease.

There is a self-consistent solution for the polar gap with a strong magnetic field, $B(s{=}\Delta R_p) > 0{\cdot}1\,B_{\rm cr}$ or $H_b > \Delta R_p$ (cf. Cheng and Ruderman 1980). The surface is heated to $T_{\rm s} \sim T_e$, required for marginally effective thermionic emission. The number density of primary electrons, $n_{\rm prim}$, which is equal to $n_{\rm GJ}$ in the limit $E_\parallel^{\rm RS} \gg E_\parallel^{\rm ion}$ of complete ionization, is such that the difference $n_{\rm GJ} - n_{\rm prim}$ is proportional to $E_\parallel^{\rm RS} - E_\parallel^{\rm ion}$. The potential difference is just $E_\parallel^{\rm ion}$ times the height of the polar gap, which is identified as the Ruderman–Sutherland value $\frac{1}{2}\Delta R_p$. Thus this self-consistent model has

$$T_{\rm s} \simeq T_e\,, \qquad n_{\rm prim} \simeq n_{\rm GJ}(1 - E_\parallel^{\rm ion}/E_\parallel^{\rm RS})\,, \qquad \Delta\varphi \simeq \tfrac{1}{2}E_\parallel^{\rm ion}\Delta R_p\,,$$
$$E_\parallel \simeq \Theta[s]\Theta[\tfrac{1}{2}\Delta R_p - s]E_\parallel^{\rm ion}\,, \tag{5·18}$$

where $\Theta[x]$ is the step function equal to unity for $x > 0$ and zero for $x < 0$.

To obtain (5·18) we assume that none of the parameters of the polar gap depend on time. Alternatively it may be possible to find a time-dependent gap solution, analogous to the sparking model of Ruderman and Sutherland (1975). We have not explored this possibility in detail. Our preliminarily considerations suggest that such a time-dependent model may imply a somewhat higher (than our time-independent model) total power carried away by both relativistic particles and radiation from the polar gap into the pulsar magnetosphere.

Although photoionization of bound pairs occurs for $P < P_1$ it has little effect on the model (5·18) provided the number density of ionized pairs, $n_\pm$, at $s \simeq \frac{1}{2}\Delta R_p$ is smaller than $n_{\rm GJ} - n_{\rm prim} \simeq n_{\rm GJ}(E_\parallel^{\rm ion}/E_\parallel^{\rm RS})$. From (5·12) and (5·18), the equality $n_\pm = n_{\rm GJ} - n_{\rm prim}$ defines a lower limit, $P = P_2$, to the period:

$$P_2 = (0{\cdot}07\,{\rm s})\left(\frac{T_{\rm s}}{10^6\,{\rm K}}\right)^{\frac{4}{11}}\left(\frac{B_{\rm s}}{0{\cdot}1\,B_{\rm cr}}\right)^{\frac{2}{11}}. \tag{5·19}$$

For $P < P_2$ the number density of free pairs is sufficient to cause an additional screening, reducing $E_\parallel$ to $\ll E_\parallel^{\rm ion}$. Thus the model (5·18) applies only for $P_2 < P < P_1$.

For $P_2 < P < P_1$, (5·3) and (5·18) imply that the total power carried away by both relativistic particles and radiation from the polar gap into the pulsar magnetosphere is

$$L_p \simeq \pi(\Delta R_p)^2 n_{\rm prim} ce\Delta\varphi \simeq \tfrac{3}{2}\frac{E_\parallel^{\rm ion}}{E_\parallel^{\rm RS}}\left(1 - \frac{E_\parallel^{\rm ion}}{E_\parallel^{\rm RS}}\right)\dot{E}_{\rm rot}\,, \tag{5·20}$$

where (e.g., Ostriker and Gunn 1969)

$$\dot{E}_{\rm rot} \simeq \frac{2\pi\Omega^4 R^6 B_{\rm s}^2}{3\mu_0 c^3} \simeq (1{\cdot}8\times10^{29}\,{\rm W})\left(\frac{P}{0{\cdot}1\,{\rm s}}\right)^{-4}\left(\frac{B_{\rm s}}{0{\cdot}1\,B_{\rm cr}}\right)^2 \tag{5·21}$$

is the rate of rotation energy loss of the neutron star. The maximum conceivable value of the energy flux in nonthermal particles is $\dot{E}_{\rm rot}$. This maximum is achieved (to within a factor of order unity) in the Sturrock model with

$L_p \simeq \pi(\Delta R_p)^2 n_{\rm prim} ce\Delta\varphi$ in (5·20) interpreted in terms of $n_{\rm prim} = n_{\rm GJ}$, cf. (2·1), and $\Delta\varphi = \Delta\varphi_{\rm max}$, cf. (1·1). However, as already remarked, the Sturrock model is not internally consistent. We now argue that the modified model (5·18) can produce L_p close to this maximum.

It is convenient to define the ratio $\eta_\gamma^b = L_p/\dot{E}_{\rm rot}$ of the spin-down power going into primary particles. In our modified model this fraction is given by

$$\eta_\gamma^b = \frac{L_p}{\dot{E}_{\rm rot}} \simeq \tfrac{3}{2}\frac{E_\parallel^{\rm ion}}{E_\parallel^{\rm RS}}\left(1 - \frac{E_\parallel^{\rm ion}}{E_\parallel^{\rm RS}}\right) \quad \text{at} \quad P_2 < P < P_1\,. \tag{5·22}$$

Equations (5·16) and (5·22) yield

$$\eta_\gamma^b \simeq \tfrac{3}{2}\left(\frac{P}{P_1}\right)^{\frac{3}{2}}\left[1 - \left(\frac{P}{P_1}\right)^{\frac{3}{2}}\right] \quad \text{at} \quad P_2 < P < P_1\,. \tag{5·23}$$

The value of η_γ^b has a maximum, $\eta_\gamma^b = \frac{3}{8}$, at $P = 2^{-\frac{2}{3}} P_1 \simeq 0{\cdot}6\,P_1$.

For comparison with (5·22) or (5·23), suppose that both ejection of particles from the pulsar surface is limited and pairs are created free. Then the fraction of the spin-down power radiated by pulsars is (Ruderman and Sutherland 1975; Cheng and Ruderman 1980)

$$\eta_\gamma^f \simeq 1{\cdot}5 \times 10^{-3}\left(\frac{B_{\rm s}}{0{\cdot}1\,B_{\rm cr}}\right)^{-\frac{8}{7}}\left(\frac{P}{0{\cdot}1\,{\rm s}}\right)^{\frac{15}{7}}. \tag{5·24}$$

From (5·22) and (5·24) we can see that for $B_{\rm s} \simeq (0{\cdot}1\text{–}1)B_{\rm cr}$ the ratio $\eta_\gamma^b/\eta_\gamma^f$ is $\sim$20 at $P = 0{\cdot}6\,P_1$ and $\sim 10^2$ at $P = P_2$. Hence, at $P_2 < P < P_1$ the nonthermal luminosity of pulsars with strong magnetic fields is considerably enhanced as a result of the creation of bound pairs instead of free pairs. The nonthermal luminosity of such a pulsar with $P \simeq 0{\cdot}6\,P_1$ may be comparable with the spin-down power, as in the model of Sturrock (1971).

The model (5·18) breaks down for $P < P_2$ and for $P > P_1$. Consider the lower limit, $P = P_2$. According to (5·12) with (2·1), the density of free pairs resulting from field ionization increases with decreasing pulsar period, $n_\pm \propto P^{-5}$, and for $P < P_2$ the number density of ionized pairs dominates in the screening of $E_\parallel$, thereby reducing $\Delta\varphi$ in (5·18) and hence L_p according to (5·19). The fraction of the spin-down power radiated by pulsars drops sharply from $\sim \eta_\gamma^b$ for $P > P_2$ to $\sim \eta_\gamma^f$ for $P \ll P_2$. For $P > P_1$ and $T_{\rm s} < T_e$, there is neither particle ejection from the pulsar surface nor a cascade of pair production in the polar gaps. In this case the nonthermal luminosity of pulsars is negligible. Hence, for pulsars with strong magnetic fields, the death line should be $P = P_1$ (cf. Chen and Ruderman 1993). However, this predicted death line is not supported by observation, as discussed further in Section 5·5 below.

5·3 The Case $\boldsymbol{\Omega}\cdot\mathbf{B} < 0$ at the Polar Caps

Ions tend to be extracted from the stellar surface in the polar caps of pulsars by any parallel electric field in the case $\boldsymbol{\Omega}\cdot\mathbf{B} < 0$. As for models with $\boldsymbol{\Omega}\cdot\mathbf{B} > 0$, it is convenient to distinguish between the case where particles can flow freely from the surface due to thermionic emission, and the case where flow from the

surface is limited. The discussion of these two cases closely parallels those in Sections 5·1 and 5·2, respectively.

Ions flow freely from the pulsar surface with density $\sim n_{\rm GJ}$ if the temperature of the polar cap satisfies $T_{\rm s} > T_i$, cf. (2·17). The potential, $\Delta\varphi$, near the pulsar surface then cannot be much greater than $\Delta\varphi_{\rm RS}$. The point is that for both $\Delta\varphi > \Delta\varphi_{\rm RS}$ and $H > H_i$, cf. (5·13), the polar gap is unstable, in the sense that a cascade of pair production develops. The cascade is stopped only when either the potential becomes of order $\Delta\varphi_{\rm RS}$ or the thickness of the polar gap becomes $\sim H_i$ when the photoionization of bound pairs is small. It follows from the discussion in Section 5·1 that for $H < H_f$, the potential across the polar gap is not much greater than $\Delta\varphi_{\rm RS}$ for any known pulsar. Any increase (due to the reduced screening resulting from the pairs being bound rather than free) in the energy flux in particles is at most modest. Hence, for free ejection of ions from the polar cap, the creation of bound pairs in a strong magnetic field cannot be responsible for the high-frequency radiation of pulsars.

Provided that the temperature of the polar cap, $T_{\rm s}$, without heating by reversed electrons is smaller than T_i, thermionic emission of ions is negligible. The $E_\parallel$ field distribution near the polar cap is then given by (5·15). As for the case described in Section 5·2, for $P < P_1$, one has $E_\parallel > E_\parallel^{\rm ion}$ and the potential $\Delta\varphi$ across the polar gap is substantially greater than the Ruderman–Sutherland limit, $\Delta\varphi_{\rm RS} \simeq$ a few $\times 10^{12}$ V. Such a gap is unstable to pair production inside it. Indeed, if a pair is created inside the gap, the field $E_\parallel$ accelerates the positron out of the gap and accelerates the electron toward the stellar surface. Since $\Delta\varphi > \Delta\varphi_{\rm RS}$, one (or both) of these particles is accelerated in the gap until it generates the curvature radiation which is absorbed inside the gap to create secondary pairs. The total number of such secondary pairs per primary particle is much greater than unity. With $E_\parallel > E_\parallel^{\rm ion}$ these pairs are necessarily free. In turn, the secondary pairs are accelerated and generate curvature photons which are absorbed to create tertiary pairs and so on. This cascade ceases if the temperature of the polar cap is heated by reversed electrons so that the surface temperature increases up to $\sim T_i$. (One has $T_i < T_{\rm RS}$, cf. (5·17), and the heating can increase the surface temperature to $T_{\rm RS}$.) Then outflowing ions screen $E_\parallel$, restricting it to $E_\parallel \sim (1\text{–}2)E_\parallel^{\rm ion}$. Our modified polar gap, summarized in (5·18), then applies, with T_e replaced by T_i and with $n_{\rm prim}$ the sum of the density of outflowing ions and of the positrons created in the polar gap. Thus, (5·20) may be used to estimate the total power carried away by both relativistic particles and radiation from the polar gap into the pulsar magnetosphere.

5·4 Interpretation of Observational Data

Strong nonthermal radiation in X-rays and γ-rays has been observed from a few radio pulsars (Gunji *et al.* 1994; Ulmer 1994). Some observational data and theoretical predictions on these pulsars are presented in Table 1.

The strength of the magnetic field given in Table 1 is estimated from the slow down of the pulsar rotation ($B_{\rm s} \propto (P\dot{P})^{\frac{1}{2}}$). This actually estimates the value of the magnetic field near the light cylinder (the inner boundary of the radiation zone). The strength of the magnetic field at the stellar surface depends on the assumption about the structure of the magnetic field, which is assumed dipolar. Thus, in Table 1, for each pulsar it is the dipole component of the magnetic field

Table 1. Properties of high-frequency pulsars with data taken from Ulmer (1994)
The distances to PSR 1706–44, from Taylor, Manchester and Lyne (1993), and to PSR 1055–52, from Koribalski (1995), are indicated in parentheses

Name	P (ms)	B_s (10^8 T)	D (kpc)	$L_{X+\gamma}$ (10^{29}W)	$\dot{E}_{rot}$ (10^{29} W)	η_γ^{obs} (10^{-2})	η_γ^f 10^{-2}	η_γ^b 10^{-2}
PSR 0531+21	33	6·6	2	2·2	450	0·5	0·01	1·7
PSR 0540–69	50	9	55	0·9	150	0·6	0·02	2·3
PSR 0833–45	89	6·8	0·5	0·084	7	1·2	0·08	4·6
PSR 1706–44	102	6·3	2·8	0·084	3·4	9	0·1	6
PSR 1509–58	150	31	4·2	0·39	20	2	0·04	3·6
PSR 1055–52	197	2	1·8	0·006	0·03	80	1	—
		(6)						22
Geminga	237	3·3	(0·15)	0·003	0·035	9	1	—
		(6)						27

at the magnetic pole that is given. These values of B_s are twice as strong as the estimates of Michel (1991), whose B-values apply to the magnetic equator, rather than to the magnetic poles which are more relevant for the polar gaps (cf. Shapiro and Teukolsky 1983).

The values of B_s given in Table 1 are lower limits on the actual surface fields. The estimated fields also depend on the angle, i, between the dipole axis and the rotaion axis, and the quoted values for $i = \pi/2$ correspond to the minimum value of the dipole moment. More importantly, the actual field may be much more complicated than a pure dipole. For example, suppose the magnetic field of a pulsar were purely quadrupolar rather than purely dipolar; then to explain the same rate of deceleration of the pulsar rotation, the surface magnetic field would need to be $(c/\Omega R) \sim 10^2$–10^4 times stronger. For PSR1055–52 and Geminga, the dipolar components give fields smaller than $0{\cdot}1\,B_{cr}$. If this were the actual field then pairs would be created free. In suggesting that bound pairs might cause an increase in the pulsar luminosity, we need to assume a surface field stronger than the dipolar value. The value $B_s \sim 6 \times 10^8$ T is indicated in parentheses for these pulsars in Table 1.

From Table 1 we can see that the following inequalities hold for all pulsars: $\eta_\gamma^f \ll \eta_\gamma^b$ and $\eta_\gamma^{obs} < \eta_\gamma^b$. We conclude that the effect of adiabatic conversion of the curvature γ-quanta into mutually bound pairs in a strong magnetic field, $B > 0{\cdot}1\,B_{cr}$, is able to increase the nonthermal luminosities of pulsars sufficiently to account for the observations. However, the condition $P > P_2$, cf. (5·19), is not satisfied for two of the pulsars listed, specifically for the Crab and the Crab-like PSR 0540–69. Apart from these two, we conclude that photoionization of bound pairs is unimportant in determining the polar-gap structure, so that (5·23) applies. Thus the nonthermal high-frequency radiation of these pulsars may be explained in terms of the modified polar-gap model which takes account of the creation of bound pairs.

The Crab-like pulsars (PSR 0531+21 and PSR 0540–69) have periods shorter than P_2. These are also young pulsars, which may not have had time to cool sufficiently (to $T_s < T_e$ or $T_s < T_i$) for our model to apply. The high-frequency radiation from these pulsars cannot be explained in terms of our modified model.

However, for these two Crab-like pulsars, the outer-gap model of Cheng *et al.* (1986*a*) seems satisfactory (e.g., Ulmer *et al.* 1994). Moreover, the γ-ray emission from the Crab-like pulsars may also be explained in terms of the slot-gap model of Arons (1983). However, the slot gap is an effective source of the energy for nonthermal radiation only for dipole-like magnetic fields. Otherwise, the total power carried away by both relativistic particles and radiation from the slot gap into the pulsar magnetosphere is suppressed by a factor of $\sim(R_c/R)(\Omega R/c)^{\frac{1}{2}}$ (Arons 1983). It is reasonable that the radius of curvature of the magnetic field lines near the surface is of order the stellar radius, $R_c \simeq R$, in which case for the Crab pulsar the total power from the slot gap is even smaller than the total power from the polar gap in the standard non-modified polar-gap models (Ruderman and Sutherland 1975; Arons 1979, 1981; Cheng and Ruderman 1980; Mestel *et al.* 1985). Therefore, the outer-gap model of Cheng *et al.* (1986*a*) which is not so sensitive to the structure of the magnetic field near the pulsar is preferable as a model of the high-frequency radiation from Crab-like pulsars.

In Table 1, to estimate the fraction, η_γ^b, of the spin-down power, $\dot{E}_{\rm rot}$, radiated by pulsars in the modified polar-gap model it is assumed that only one polar gap is a source of both high-energy particles and radiation in the pulsar magnetospheres. This assumption is reasonable for PSR 1706–44, PSR 1509–58 and PSR 1055–52 which have only one γ-ray pulse in their γ-ray light curves (e.g., Ulmer 1994). The other pulsars have two pulses in their γ-ray light curves. This indicates that in their magnetospheres both polar gaps operate as particle accelerators. In this case the actual values of η_γ^b are twice the values given in Table 1. This change strengthens the conclusion that the modified polar-gap model is able to explain the observed high-frequency luminosities of pulsars.

The distance to Geminga is particularly uncertain and the value adopted (150 pc) is also indicated in parentheses in Table 1. If the distance is less than $\sim$50 pc, we have $\eta_\gamma^{\rm obs} \lesssim \eta_\gamma^f$, and the standard polar-gap models could describe Geminga's γ-ray and X-ray emission adequately (Harding, Ozernoy and Usov 1993). The high-frequency luminosity of Geminga may be explained in the modified polar-gap model if the distance to Geminga is up to $\sim$250 pc.

Recently, Sturner and Dermer (1994) and Daugherty and Harding (1994) have shown that double pulses with large interpulse separations seen in the Crab, Vela, and Geminga can be produced by hollow cone emission from a single pole if the rotation and magnetic axes are nearly aligned. In these models the solid angle of γ-ray emission is very small, and the standard polar gap models have no problem supplying the power necessary to give the observed fluxes of γ-rays. However, in this case the chance of observing any given pulsar from the Earth is not more than $\sim 10^{-2}$. As noted by Daugherty and Harding (1994), in spite of the poor statistics, it seems hard to reconcile such a low probability of pulsar detection with either the fraction of γ-ray pulsars observed among the known supernova remnants, or the fraction which have a double-pulse structure.

5·5 Death Line at $P = P_1$

The prediction that $P = P_1$ should be the death line (no free pairs for $P > P_1$) for pulsars with $B \gtrsim 0{\cdot}1\, B_{\rm cr}$ is not supported by the data. The distribution of radio pulsars essentially ignores our death line. The radio emission is attributed to free pairs and hence it appears that there is some source of free pairs even for

pulsars with $B > 0{\cdot}1\,B_{\rm cr}$ and $P > P_1$. There are several possibilities within the framework of our model. One suggestion concerns the decay of positronium from the excited state formed from $\perp$-polarized photons (Section 4·3). This decay should produce some free pairs, due for example to two-photon decay (cf. Melrose and Kirk 1986) to the densely-packed states ($n_c \to \infty$) around zero binding energy for the ground state ($n = n' = 0$). Even a small branching ratio for generation of free pairs may suffice to account for the apparent lack of suppression of the radio emission. Two other possibilities for the formation of some free pairs are suggested by a critical examination of the assumption that the curvature photons emitted by the primary particles cannot decay directly into free pairs (Section 3·2). In our discussion in Section 3·2 we assume that *all* curvature photons are confined to a forward cone with half angle $\sim 1/\Gamma$. However, a small fraction, $\sim 1/\Gamma$, of the power is emitted outside this cone. Some of these photons should satisfy the condition for decay into free pairs at the point of emission, and these photons should be a source of some free pairs. Another possibility follows from the fact that for any radiation process that produces photons with energy above the threshold for pair creation, the analogous process in which the photon is replaced by a pair is allowed. Thus direct curvature emission of pairs is another possible source of free pairs. Another possibility follows from the fact that for any radiation process that produces photons with energy above the threshold for pair creation, the analogous process in which the photon is replaced by a pair is allowed. Thus direct curvature emission of pairs is another possible source of free pairs. Photon–photon production of pairs is yet a further possibility. The efficacy of these processes needs to be explored, but is subject to the major uncertainty that the number of free pairs required to account for the radio emission is poorly constrained.

We conclude that $P = P_1$ should be regarded as a death line for high-frequency emission, but not necessarily for radio emission, for which the luminosity is many orders smaller than the spin-down power. However, our arguments on this point are speculative, and a quantitative analysis is desirable.

6. Conclusions and Discussion

In this paper we consider pulsars with strong magnetic fields, $B_{\rm s} \gtrsim 0{\cdot}1\,B_{\rm cr}$, at their surfaces such that bound rather than free pairs should form due to decay of γ-rays in polar gaps. In discussing various relevant aspects of the underlying physical processes, we make the following points:

(1) The surface structure of magnetic neutron stars determines whether particles flow freely from the surface, leading to a model of the type discussed by Arons (1981, 1983), or whether particles are strongly bound to the surface, leading to a model of the type discussed by Ruderman and Sutherland (1975) and Cheng and Ruderman (1980). For pulsars with $\boldsymbol{\Omega} \cdot \mathbf{B} > 0$, the requirement on the surface temperature, $T_{\rm s}$, for electrons to remain strongly bound is $T_{\rm s} < T_e$, with T_e given by (2·13). For pulsars with $\boldsymbol{\Omega} \cdot \mathbf{B} < 0$, the requirement for ions to remain strongly bound is $T_{\rm s} < T_i$, with T_i given by (2·7).

(2) In polar-gap models the primary particles emit curvature photons which are initially at too small an angle to $\mathbf{B}$ to decay into pairs, even when the curvature drift and the polarization drift are included.

(3) For such photons emitted near the stellar surface, $s = 0$, the curvature of dipolar field lines allows decay into pairs with a minimum Lorentz factor $\Gamma_{\min}$ that decreases $\propto 1/s$ with increasing height, cf. (5·8).

(4) The photons can be either $\|$-polarized or $\perp$-polarized. If the magnetic field is strong enough, $B \gtrsim 8 \times 10^8$ T, photon splitting tends to cause the $\perp$-polarized photons to decay into $\|$-polarized photons. The formation of positronium necessarily occurs before the threshold for decay into free pairs is reached; the sole criterion for positronium formation is whether or not tunneling occurs from the lower to the upper branch of the photon–positronium dispersion curves in Fig. 1.

(5) In a moderately strong magnetic field, $B \gtrsim 4 \times 10^8$ T, photons evolve into a bound pair (positronium) rather than decaying into a free pair. The $\|$-polarized produce positronium in its ground state, and the $\perp$-polarized produce positronium in an excited state that quickly decays to the ground state through gyromagnetic emission (actually a spin-flip transition).

(6) The positronium atoms can be destroyed (a) by field ionization for $E_\| \gtrsim E_\|^{\rm ion}$, with $E_\|^{\rm ion}$ given by (4·29), or (b) by photoionization due to thermal radiation from the neutron star, with mean free path given by (4·32).

In applying these properties to polar-gap models for pulsars we distinguish between two types of model mentioned in point (1) above: models in which particles flow freely from the surface, implying $E_\| = 0$ at the surface (e.g., Arons 1981, 1983), and models in which particles are tightly bound to the surface, so that $E_\|$ has the vacuum value just above the surface (e.g., Ruderman and Sutherland 1975). The parallel electric field in the former, $E_\|^{\rm A}$ given by (3·11), is much smaller than that in the latter, $E_\|^{\rm RS}$ given by (3·12), and there is a corresponding difference in the potential drop, $\Delta\varphi \sim E_\| H$, across the polar= gap of height H. Our particular interest is in the energy flux of primary particles, which is assumed to determine the nonthermal, = high-frequency luminosity (e.g., Harding and Daugherty 1993). The energy flux of primary particles is $n_{\rm prim} c\pi \Delta R_p^2 e \Delta\varphi$, where $n_{\rm prim}$ is the number density of primaries and $\Delta R_p \simeq (\Omega R/c)^{\frac{1}{2}} R$ is the radius of the polar cap. For $n_{\rm prim} \sim n_{\rm GJ}$, cf. (2·1), and $\Delta\varphi \sim \Delta\varphi_{\max}$, cf. (1·1), this is of order the spin-down power of the pulsar. However, Arons-type models have a small $E_\|^{\rm A} \ll E_\|^{\rm RS}$, Ruderman–Sutherland-type models have small $H \ll \Delta R_p$, and both have $\Delta\varphi \ll \Delta\varphi_{\max}$, so that the power in primary particles is severely limited. The formation of positronium, rather than free pairs tends to reduce the screening of $E_\|$, and hence to increase H.

We find the following specific results for models in which bound pairs are formed.

(7) There is at most a modest increase in the power in primary particles in Arons-type models, and even after modification to include positronium formation, these models cannot account for the observed high-frequency emission.

(8) In the Ruderman–Sutherland-type models, the formation of bound pairs can have a large effect on the model, greatly increasing the height of the polar gap. This model requires $T_{\rm s} < T_e$ or $T_{\rm s} < T_i$, cf. point (1) above, and then photoionization of the bound pairs is unimportant.

(9) For $P > P_1$, cf. (5·16), corresponding to $E_\|^{\rm RS} < E_\|^{\rm ion}$, cf. point (6) above, there is no field ionization of the bound pairs. This suggests that $P = P_1$ should be the death line for pulsars with $B > 0{\cdot}1\, B_{\rm cr}$. Observationally, radio pulsars

seem to ignore this death line. In Section 5·5 we suggest processes that should produce some free pairs even for $P > P_1$, and note that only a modest number of pairs is required to account for the radio emission.

(10) For $P_2 < P < P_1$ we argue for a self-consistent model in which field ionization generates just enough free pairs for the reverse flux of primary particles to heat the polar cap sufficiently to maintain thermionic emission at the rate required for partial screening to reduce $E_\parallel$ from $E_\parallel^{\rm RS}$ to $\sim E_\parallel^{\rm ion}$. This model is summarized in (5·18). The modified model is only weakly dependent on whether electrons or ions are pulled from the stellar surface; for ions, replace T_e in (5·18) by T_i.

(11) For $P < P_2$, cf. (5·19), the number density of pairs from the field ionization exceeds the number density of primaries, and with decreasing P the model rapidly approaches that without bound-pair formation.

(12) In the modified model the ratio, η_γ^b, of the power in primary particles to the spin-down power, cf. (5·23), can be close to unity. In this sense the model is similar to that of Sturrock (1971), but without the internal inconsistency in the Sturrock model.

In summary, the most important modifications due to the formation of bound pairs rather than free pairs is for pulsars with strong surface magnetic fields, $B_{\rm s} \gtrsim 4 \times 10^8\,{\rm T}$, with cool surfaces, $T_{\rm s} \lesssim 5 \times 10^5\,{\rm K}$, and periods in the range $P_2 < P < P_1$. The model proposed here could then account for the efficient high-frequency emission.

The high-frequency pulsars are (Table 1) PSR 0531+21 (the Crab), PSR 0540–69, PSR 0833–45 (Vela), PSR 1706–44, PSR 1509–58, PSR 1055–52 and Geminga. Of these, the middle three satisfy all the requirements for our modified model, but the first two (Crab-like) pulsars have periods $P < P_2$ and the last two have surface magnetic fields $B_{\rm s} < 4 \times 10^8\,{\rm T}$. For the Crab-like pulsars, the photoionization of bound pairs inside the polar gaps should be strong, and the modified polar-gap model is then not applicable. The outer-gap model of (Cheng, Ho and Ruderman 1986*a*) seems a viable alternative for these Crab-like pulsars (e.g., Ulmer *et al.* 1994). We argue that the magnetic field is likely to have nondipolar components and these are not included in the estimate of $B_{\rm s}$ in Table 1. With plausible values for a nondipolar component, the model may also apply to PSR 1055–52 and Geminga. Recently, Usov (1994) has shown that the outer-gap model of Cheng, Ho and Ruderman (1986*b*) is inconsistent with the available data on Geminga, implying a polar-gap model. For Geminga the actual distance is important in estimating whether or not the modified polar-gap model is viable, as discussed in Section 5·4. Alternatively, Harding, Ozernoy and Usov (1993) argued that, provided the distance to Geminga is not more than ~40–50 pc, it is possible to explain both the X-rays and γ-rays in terms of the polar-gap model of Arons (1979, 1981).

We discuss some other details of the application to high-frequency pulsars elsewhere (Usov and Melrose 1995). We conclude by commenting on the polarization of the high-frequency radiation. According to (4) above, for $B_{\rm s} \gtrsim 0{\cdot}2\,B_{\rm cr}$, most of the $\perp$-polarized photons with $\varepsilon_\gamma \lesssim 10^2\,{\rm MeV}$ produced by curvature mechanism near the pulsar surface, are split and transformed into $\parallel$-polarized photons before the pair creation threshold is reached (Section 4·2). As a result, the γ-ray emission recorded from the pulsar at energies $\varepsilon_\gamma \lesssim 10^2\,{\rm MeV}$ should be linearly polarized. Near the maximum of the light curve, the γ-ray polarization may be

as high as 100%. The degree of γ-ray polarization should decrease toward the edges of the γ-ray pulses. This is because the emission zone recedes from the neutron star surface as the phase of γ-ray emission shifts from the maximum of the light curve, implying that the B value in the line of sight to the region of γ-ray generation decreases. By observing the polarization of the γ-ray emission of pulsars it would be possible to estimate the strength of the magnetic field near the pulsar surface.

Acknowledgments

VVU is grateful to Jonathan Arons, Charles Dermer, Alice Harding, Curtis Michel and Steve Sturner for helpful conversations. DBM thanks Simon Johnston and Jean Eilek for helpful comments.

References

Abrahams, A. M., and Shapiro, S. L. (1991). Equation of state in a strong magnetic field: finite temperature and gradient corrections *Astrophys. J.* **374**, 652–667.

Adler, S. L. (1971). Photon splitting and photon dispersion in a strong magnetic field *Ann. Phys.* **67**, 599–647.

Adler, S. L., Bahcall, J. N., Callan, C. G., and Rosenbluth, M. N. (1970). Photon splitting in a strong magnetic field *Phys. Rev. Lett.* **25**, 1061–1065.

Arons, J. (1979). Some problems of pulsar physics *Space Sci. Rev.* **24**, 437–510.

Arons, J. (1981). Pair creation above pulsar polar caps: steady flow in the surface acceleration zone and polar cap X-ray emission *Astrophys.* **248**, 1099–1116.

Arons, J. (1983). Pair creation above pulsar polar caps: Geometrical structure and energetics of slot gaps *Astrophys. J.* **266**, 215–241.

Arons, J., and Scharlemann, E. T. (1979). Pair formation above polar caps: structure of the low altitude acceleration zone *Astrophys. J.* **231**, 854–79.

Baring, M. G. (1991). Signatures of magnetic photon splitting in gamma-ray burst spectra *Astron. Astrophys.* **249**, 581–588.

Beskin, V. S. (1982). Dynamic screening of the acceleration region in the magnetosphere of a pulsar *Soviet Astron. AJ* **26**, 443–446.

Beskin, V. S., Gurevich, A. V., and Istomin, Ya. N. (1986). Physics of pulsar magnetospheres *Soviet Phys. USP.* **29**, 946–970.

Bhatia, V. B., Chopra, N., and Panchapakesan, N. (1988). The effect of photon capture and field ionisation on high magnetic field pulsars *Astrophys. Space Sci.* **150**, 181–188.

Bhatia, V. B., Chopra, N., and Panchapakesan, N. (1992). Photodissociation in strong magnetic fields and application to pulsars *Astrophys. J.* **388**, 131–137.

Bialynicka-Birula, Z., and Bialynicki-Birula, I. (1970). Nonlinear effects in quantum electrodynamics. Photon propagation and photon splitting in an external field *Phys. Rev.* **D2**, 2341–2345.

Bogovalov, S. V., and Kotov, Yu.D. (1989). Electromagnetic cascade in a pulsar magnetosphere, and the processes on the neutron star surface *Soviet Astron. Lett.* **15**, 185–189.

Chen, H.-H., Ruderman, M. A., and Sutherland, P. G. (1974). Structure of solid iron in superstrong neutron-star magnetic fields *Astrophys. J.* **191**, 473–477.

Chen, K., and Ruderman, M. A. (1993). Pulsar death lines and death valley *Astrophys. J.* **402**, 264–270.

Cheng, A. F., and Ruderman, M. A. (1977). Pair-production discharges above pulsar polar caps *Astrophys. J.* **214**, 598–606.

Cheng, A. F., and Ruderman, M. A. (1980). Particle acceleration and radio emission above pulsar polar caps *Astrophys. J.* **235**, 576–586.

Cheng, K. S., Ho, C., and Ruderman, M. A. (1986*a*). Energetic radiation from rapidly spinning pulsars. I. Outer magnetosphere gaps *Astrophys. J.* **300**, 500–521.

Cheng, K. S., Ho, C., and Ruderman, M. A. (1986*b*). Energetic radiation from rapidly spinning pulsars. II. Vela and Crab *Astrophys. J.* **300**, 522–539.

Daugherty, J. K., and Ventura, J. (1978). Absorption of radiation by electrons in intense magnetic fields *Phys. Rev.* **D18**, 1053.
Erber, T. (1966). High-energy electromagnetic conversion processes in intense magnetic fields *Rev. Mod. Phys.* **38**, 626–659.
Fitzpatrick, R., and Mestel, L. (1988*a* & *b*). Pulsar electrodynamics—I & II *Mon. Not. R. Astron. Soc.* **232**, 277–302 & 303–321.
Flowers, E. G., Lee, J.-F., Ruderman, M. A., Sutherland, P. G., Hillebrandt, W., and Müller, E. (1977). Variation calculation of ground-state energy of iron atoms and condensed matter in strong magnetic fields *Astrophys. J.* **215**, 291–301.
Fushiki, I., Gudmundsson, E. H., and Pethick, C. J. (1989). Surface structure of neutron stars with high magnetic fields *Astrophys. J.* **342**, 958–975.
Ginzburg, V. L., and Usov, V. V. (1972). Concerning the atmosphere of magnetic neutron stars (pulsars) *JETP Lett.* **15**, 196–198.
Goldreich, P., and Julian, W. H. (1969). Pulsar electrodynamics *Astrophys. J.* **157**, 869–880.
Gopal, E. S. R. (1974). *Statistical Mechanics and Properties of Matter* (New York: Wiley).
Gunji, S., *et al.* (1994). Observation of pulsed hard X-rays/γ-rays from PSR 1509–58 *Astrophys. J.* **428**, 284–291.
Halpern, J. P., and Holt, S. S. (1992). Discovery of soft X-ray pulsations from the γ-ray source Geminga *Nature* **357**, 222–224.
Harding, A., and Daugherty, J. K. (1993). Pulsar gamma-ray emission in the polar cap cascade model in Van Riper, K. A., Epstein, R., and Ho, C. (eds) *Isolated Pulsars* (Cambridge University Press), pp. 279–286.
Harding, A., Ozernoy, L. M., and Usov, V. V. (1993). Geminga, origins of its X-ray and gamma-ray emission *Mon. Not. R. Astron. Soc.* **265**, 921–925.
Hayward, E. (1965). Photonuclear reactions in MacDonald, N. (ed.) *Nuclear Structure and Electromagnetic Interaction* (Oliver and Boyd: Edinburgh), pp. 141–209.
Herold, H., Ruder, H., and Wunner, G. (1982). Cyclotron emission in strongly magnetized plasmas *Astron. Astrophys.* **115**, 90–96.
Herold, H., Ruder, H., and Wunner, G. (1985). Can γ quanta really be captured by pulsar magnetic fields? *Phys. Rev. Lett.* **54**, 1452–1455.
Jackson, J. D. (1975). *Classical Electrodynamics*, (Wiley: New York).
Jones, P. B. (1978). Particle acceleration at the magnetic poles of a neutron star *Mon. Not. R. Astron. Soc.* **184**, 807–827.
Jones, P. B. (1979). Pair production on the pulsar magnetosphere *Astrophys. J.* **228**, 536–540.
Jones, P. B. (1985). Density-functional calculations of the cohesive energy of condensed matter in very strong magnetic fields *Phys. Rev. Lett.* **55**, 1338–1340.
Jones, P. B. (1986). Properties of condensed matter in very strong magnetic fields *Mon. Not. R. Astron. Soc.* **218**, 477–487.
Klepikov, N. P. (1954). Radiation of photons and electron–positron pairs in a magnetic field *Zh. Eksp. Teor. Fiz.* **6**, 19–35.
Koribalski, B., Johnston, S., Weisberg, W. M., and Wilson, W. (1995). HI line measurements of eight southern pulsars *Astrophys. J.* **441**, 756–64.
Landau, L. D., and Lifshitz, E. M. (1971). *The Classical Theory of Fields* (Pergamon: Oxford).
Levinson, A., and Eichler, D. (1993). Baryon purity in cosmological gamma-ray bursts as a manifestation of event horizons *Astrophys. J.* **418**, 386–390.
Lieb, E. H. (1981). Thomas–Fermi and related theories of atoms and molecules *Rev. Mod. Phys.* **53**, 603–641.
Loudon, R. (1959). One-dimensional hydrogen atom *Am. J. Phys.* **27**, 649–655.
Melrose, D. B. (1983). Quantum electrodynamics in strong magnetic fields. II. Photon fields and interactions *Aust. J. Phys.* **36**, 775–798.
Melrose, D. B., and Kirk, J. G. (1986). Two-photon emission in X-ray pulsars 1. Basic formulas *Astron. Astrophys.* **156**, 268–276.
Melrose, D. B., and Parle, A. J. (1983). Quantum electrodynamics in strong magnetic fields. I. Electron states *Aust. J. Phys.* **36**, 755–774.
Melrose, D. B., and Zheleznyakov, V. V. (1981). Quantum theory of cyclotron emission and the X-ray line in Her X-1 *Astron. Astrophys.* **95**, 86–93.
Mestel, L. (1981). Structure of the pulsar magnetosphere W. Sieber and R. Wielebinski (eds) *Pulsars*. IAU Symposium No. 95 (Reidel: Dordrecht), pp. 9–23.

Mestel, L. (1993). Pulsar magnetospheres in Blandford, R. D., Hewish, A., and Mestel, L. (eds) *Pulsars as Physics Laboratories* (Oxford University Press), pp. 93–104.
Mestel, L., Robertson, J. A., Wang, Y.-M., and Westfold, K. C. (1985). The axisymmetric pulsar magnetosphere *Mon. Not. R. Astron. Soc.* **217**, 443–484.
Mészáros, P. (1992). *High-Energy Radiation from Magnetized Neutron Stars* (Univ. of Chicago Press).
Michel, F. C. (1975). Composition of the neutron star surface in pulsar models *Astrophys. J.* **198**, 683–685.
Michel, F. C. (1991). *Theory of Neutron Star Magnetospheres* (Univ. Chicago Press).
Müller, E. (1984). Variation calculation of iron and helium atoms and molecular chains in superstrong magnetic fields *Astron. Astrophys.* **130**, 415–418.
Neuhauser, D., Koonin, S. E., and Langanke, K. (1987). Hartree–Fock calculations of atoms and molecular chains in strong magnetic fields *Phys. Rev.* **A36**, 4163–4175.
Neuhauser, D., Langanke, K., and Koonin, S. E. (1986). Hartree–Fock calculations of atoms and molecular chains in strong magnetic fields *Phys. Rev.* **A33**, 2084–2086.
Ochelkov, Yu.P., and Usov, V. V. (1980). Curvature radiation of relativistic particles in the magnetosphere of pulsars *Astrophys. Space Sci.* **69**, 439–460.
Ogata, S., and Ichimaru, S. (1990). Electric and thermal conductivities of quenched neutron star crusts *Astrophys. J.* **361**, 511–513.
Ostriker, J. P., and Gunn, J. E. (1969). On the nature of pulsars: I. Theory *Astrophys. J.* **157**, 1395–1417.
Ozernoy, L. M., and Usov, V. V. (1977). The nature of pulsar gamma rays *Soviet Astron. AJ* **21**, 425–431.
Page, D., and Applegate, J. H. (1992). The cooling of neutron stars by direct URCA process *Astrophys. J.* **394**, L17–L20.
Pavlov, G. G., and Mészáros, P. (1993). Finite-velocity effects on atoms in strong magnetic fields and implications for neutron star atmospheres *Astrophys. J.* **416**, 752–761.
Rosen, L. C., and Cameron, A. G. W. (1972). Surface composition of magnetic neutron stars *Astrophys. Space Sci.* **15**, 137–152.
Rozental, I. L., and Usov, V. V. (1985). Cascade processes in the surface layers of pulsars *Astrophys. Space Sci.* **109**, 365–371.
Ruderman, M. A. (1971). Matter in superstrong magnetic fields: The surface of a neutron star *Phys. Rev. Lett.* **27**, 1306–1308.
Ruderman, M. A., and Sutherland, P. G. (1975). Theory of pulsars: polar gaps, sparks, and coherent microwave radiation *Astrophys. J.* **196**, 51–72.
Schiff, L. I., and Snyder, H. (1939). Theory of the quadratic Zeeman effect *Phys. Rev.* **55**, 59–63.
Schmidt, G. (1966). *Physics of High Temperature Plasmas* (Academic Press: New York).
Shabad, A. E. (1975). Photon dispersion in a strong magnetic field *Ann. Phys.* **90**, 166–195.
Shabad, A. E. (1992). *Polarization of the Vacuum and a Quantum Relativistic Gas in an External Field* (Nova Science: New York).
Shabad, A. E., and Usov, V. V. (1982). γ-Quanta capture by magnetic field and pair creation suppression in pulsars *Nature* **295**, 215–217.
Shabad, A. E., and Usov, V. V. (1984). Propagation of γ-radiation in strong magnetic fields of pulsars *Astrophys. Space Sci.* **102**, 327–358.
Shabad, A. E., and Usov, V. V. (1985). Gamma-quanta conversion into positronium atoms in a strong magnetic field *Astrophys. Space Sci.* **117**, 309–325.
Shabad, A. E., and Usov, V. V. (1986). Photon dispersion in a strong magnetic field with positronium formation: theory *Astrophys. Space Sci.* **128**, 377–409.
Shapiro, S. L., and Teukolsky, S. A. (1983). *Black Holes, White Dwarfs and Neutron Stars: The Physics of Compact Objects* (Wiley: New York).
Shibata, S. (1991). Magnetosphere of the rotation-powered pulsar: a DC circuit model *Astrophys. J.* **378**, 239–254.
Skjervold, J. E., and Östgaard, E. (1984*a*). Hydrogen and helium atoms in superstrong magnetic fields *Phys. Scripta* **29**, 448–455.
Skjervold, J. E., and Östgaard, E. (1984*b*). Heavy atoms in superstrong magnetic fields *Phys. Scripta* **29**, 543–550.
Slattery, W. L., Doolen, G. D., and DeWitt, H. E. (1980). Improved equation of state for the classical one-component plasma *Phys. Rev.* **A21**, 2087–2095.

Stoneham, R. J. (1979). Photon splitting in the magnetized vacuum *J. Phys.* **A12**, 2187–2203.
Sturrock, P. A. (1971). A model of pulsars *Astrophys. J.* **164**, 529–556.
Taylor, J. H., Manchester, R. N., and Lyne, A. G. (1993). Catalog of 558 pulsars *Astrophys. J. Suppl.* **88**, 529–568.
Toll, J. S. (1952). PhD dissertation, Princeton University.
Tsai, W., and Erber, T. (1974). Photon pair production in intense magnetic fields *Phys. Rev.* **D10**, 492–499.
Ulmer, M. P. (1994). Gamma-ray observations of pulsars *Astrophys. J. Suppl.* **90**, 789–795.
Ulmer, M. P., *et al.* (1994). OSSE observations of the Crab pulsar *Astrophys. J.* **432**, 228–238.
Usov, V. V. (1994). Radiation from Vela-like pulsars near the death line *Astrophys. J.* **427**, 394–399.
Usov, V. V. and Melrose, D. B. (1995). Bound pair creation in polar gaps and X-ray and gamma-ray emission from radio pulsars *Astrophys. J.* (submitted).
Usov, V. V., and Shabad, A. E. (1983). The decay of curvature gamma-ray photons near a neutron star surface *Soviet Astron. Lett.* **9**, 212–214.
Usov, V. V., and Shabad, A. E. (1985). Photopositronium in the magnetosphere of a pulsar *JETP Lett.* **42**, 19–23.
Van Riper, K. A. (1991). Neutron star thermal evolution *Astrophys. J. Suppl.* **75**, 449–462.
Von Neumann, J., and Wigner, E. (1964). On the behavior of eignenvalues in adiabatic processes in R. S. Knox and A. Gold (eds) *Symmetry in Solid State* (Benjamin: New York), pp. 167–172.
Woosley, S. E., and Baron, E. (1992). The collapse of white dwarfs to neutron stars *Astrophys. J.* **391**, 228–235.
Wunner, G., and Herold, H. (1979). Decay of positronium in strong magnetic fields *Astrophys. Space Sci.* **63**, 503–509.
Zheleznyakov, V. V., and Shaposhnikov, V. E. (1979). Absorption of curvature radiation *Aust. J. Phys.* **32**, 49–59.

Appendix A: Pitch-angles in the Drift Frame

To estimate the angle $\tilde{\psi}$ between the particle velocity $\tilde{\mathbf{v}}$ and the magnetic field $\tilde{\mathbf{B}}$ for a relativistic electron in its lowest Landau level, let us first consider the nonrelativistic motion of electrons in crossed $\mathbf{B}$ and $\mathbf{E}_\perp(t)$ fields. The polarization drift (e.g., Schmidt 1966; Landau and Lifshitz 1971) implies a drift $(e/m\omega_B^2)\, d\mathbf{E}_\perp(t)/dt$. For a relativistic electron in its lowest Landau orbital, the polarization drift may be obtained by making a Lorentz transformation from the rest frame. The momentum in the drift frame is

$$\tilde{p}_{\rm pd} = \frac{e}{\omega_B^2}\left(\frac{dE_\perp}{dt}\right)_c , \tag{A1}$$

where $(dE_\perp/dt)_c$ is to be evaluated in the frame in which the electron is at rest on the average. With $(E_\perp)_c = \Gamma E_\perp$ and $(dz)_c = \Gamma^{-1} dz$ (e.g., Landau and Lifshitz 1971), we have

$$\left(\frac{dE_\perp}{dt}\right)_c = c\Gamma^2 \frac{dE_\perp}{dz} . \tag{A2}$$

From (A1) and (A2), we obtain

$$\tilde{\psi} \simeq \frac{\tilde{p}_{\rm pd}}{\tilde{p}} \leq \frac{m\Gamma}{eB^2}\frac{dE_\perp}{dz} , \tag{A3}$$

where $\tilde{p} \simeq mc\Gamma$ is the particle momentum in the drift frame.

Appendix B: Minimum Energy of Created Pairs

Let us consider a neutron star with a centred magnetic dipole moment, μ. In cylindrical coordinates z, ρ, φ, the components of $\mathbf{B}$ near the polar cap are

$$B_z \simeq \frac{\mu_0}{4\pi}\frac{2\mu}{z^3}, \qquad B_\rho \simeq \frac{\mu_0}{4\pi}\frac{3\mu\rho}{z^4}, \qquad B_\varphi = 0, \tag{B1}$$

where μ is the magnetic moment, the z-axis is directed along the magnetic axis, z is measured from the neutron star centre, ρ is the distance to the magnetic axis, and φ is the azimuthal coordinate. The magnetic field lines are determined by integrating

$$\frac{dz}{B_z} = \frac{d\rho}{B_\rho}, \tag{B2}$$

which with (B1) and (B2) gives

$$\rho = \rho_0 (z/z_0)^{\frac{3}{2}}, \tag{B3}$$

where $\rho_0/z_0^{\frac{3}{2}}$ is a constant. [The exact result is $\rho = (\rho_0/z_0^{\frac{3}{2}})(\rho^2 + z^2)^{\frac{3}{2}}$.]

For a curvature photon which is emitted at the point with $z = z_0$ and $\rho = \rho_0$ along the magnetic field, $\mathbf{K} \parallel \mathbf{B}$, the angle between the wave vector $\mathbf{K}$ and the magnetic field $\mathbf{B}$ in the process of the photon propagation is

$$\vartheta(z) = \left(\frac{d\rho}{dz}\right)_0 - \left(\frac{d\rho}{dz}\right) = \frac{3}{2}\frac{\rho_0 (z^{\frac{1}{2}} - z_0^{\frac{1}{2}})}{z_0^{\frac{3}{2}}}. \tag{B4}$$

Taking into account that $\rho_0 \leq (\Omega R/c)^{\frac{1}{2}} R$ for open magnetic field lines near the polar caps of pulsars, $z \geq R$ and $z - R \ll R$, (B4) gives

$$\vartheta(z) \leq \frac{3}{4}\left(\frac{\Omega R}{c}\right)^{\frac{1}{2}} \frac{z - R}{z}. \tag{B5}$$

At a distance s from the pulsar surface, with $s \simeq z - R$, we have

$$\vartheta(s) \leq \frac{3}{4}\left(\frac{\Omega R}{c}\right)^{\frac{1}{2}} \frac{s}{R}. \tag{B6}$$

If the energy of curvature photons, ε_γ, is smaller than

$$\varepsilon_{\min} = 2mc^2/\vartheta, \tag{B7}$$

the process of pair creation by these photons is kinematically forbidden. From (B6) and (B7) it follows that the Lorentz factor of particles which can be created at the distance s exceeds

$$\Gamma_{\min} = \frac{\varepsilon_{\min}}{2mc^2} = \frac{4}{3}\left(\frac{c}{\Omega R}\right)^{\frac{1}{2}} \frac{R}{s}. \tag{B8}$$

Manuscript received 4 November 1994, accepted 17 March 1995